



## Nighttime observation and chemistry of HO<sub>x</sub> in the Pearl River Delta and Beijing in summer 2006

K. D. Lu<sup>1,2</sup>, F. Rohrer<sup>2</sup>, F. Holland<sup>2</sup>, H. Fuchs<sup>2</sup>, T. Brauers<sup>2</sup>, A. Oebel<sup>2,\*</sup>, R. Dlugi<sup>3</sup>, M. Hu<sup>1</sup>, X. Li<sup>1,2</sup>, S. R. Lou<sup>2,4,\*\*</sup>, M. Shao<sup>1</sup>, T. Zhu<sup>1</sup>, A. Wahner<sup>2</sup>, Y. H. Zhang<sup>1</sup>, and A. Hofzumahaus<sup>2</sup>

<sup>1</sup>State Key Joint Laboratory of Environmental Simulation and Pollution Control, College of Environmental Sciences and Engineering, Peking University, Beijing, China

<sup>2</sup>Institut für Energie und Klimaforschung: Troposphäre, Forschungszentrum Jülich, Jülich, Germany

<sup>3</sup>Arbeitsgruppe Atmosphärische Prozesse (AGAP), Munich, Germany

<sup>4</sup>School of Environmental Science and Technology, Shanghai Jiao Tong University, Shanghai, China

\* now at: Carl Zeiss SMS GmbH, Jena, Germany

\*\* now at: Shanghai Academy Of Environmental Sciences, Shanghai, China

Correspondence to: Y. H. Zhang (yhzhang@pku.edu.cn) and A. Hofzumahaus (a.hofzumahaus@fz-juelich.de)

Received: 11 October 2013 – Published in Atmos. Chem. Phys. Discuss.: 2 December 2013

Revised: 28 March 2014 – Accepted: 28 March 2014 – Published: 21 May 2014

**Abstract.** Nighttime HO<sub>x</sub> chemistry was investigated in two ground-based field campaigns (PRIDE-PRD2006 and CAREBEIJING2006) in summer 2006 in China by comparison of measured and modeled concentration data of OH and HO<sub>2</sub>. The measurement sites were located in a rural environment in the Pearl River Delta (PRD) under urban influence and in a suburban area close to Beijing, respectively. In both locations, significant nighttime concentrations of radicals were observed under conditions with high total OH reactivities of about 40–50 s<sup>-1</sup> in PRD and 25 s<sup>-1</sup> near Beijing. For OH, the nocturnal concentrations were within the range of (0.5–3) × 10<sup>6</sup> cm<sup>-3</sup>, implying a significant nighttime oxidation rate of pollutants on the order of several ppb per hour. The measured nighttime concentration of HO<sub>2</sub> was about (0.2–5) × 10<sup>8</sup> cm<sup>-3</sup>, containing a significant, model-estimated contribution from RO<sub>2</sub> as an interference. A chemical box model based on an established chemical mechanism is capable of reproducing the measured nighttime values of the measured peroxy radicals and k<sub>OH</sub>, but underestimates in both field campaigns the observed OH by about 1 order of magnitude. Sensitivity studies with the box model demonstrate that the OH discrepancy between measured and modeled nighttime OH can be resolved, if an additional RO<sub>x</sub> production process (about 1 ppb h<sup>-1</sup>) and additional recycling (RO<sub>2</sub> → HO<sub>2</sub> → OH) with an efficiency equivalent to 1 ppb NO is assumed. The additional recycling mechanism was

also needed to reproduce the OH observations at the same locations during daytime for conditions with NO mixing ratios below 1 ppb. This could be an indication that the same missing process operates at day and night. In principle, the required primary RO<sub>x</sub> source can be explained by ozonolysis of terpenoids, which react faster with ozone than with OH in the nighttime atmosphere. However, the amount of these highly reactive biogenic volatile organic compounds (VOCs) would require a strong local source, for which there is no direct evidence. A more likely explanation for an additional RO<sub>x</sub> source is the vertical downward transport of radical reservoir species in the stable nocturnal boundary layer. Using a simplified one-dimensional two-box model, it can be shown that ground-based NO emissions could generate a large vertical gradient causing a downward flux of peroxy acetic nitrate (PAN) and peroxyacetyl nitrate (MPAN). The downward transport and the following thermal decomposition of these compounds can produce up to 0.3 ppb h<sup>-1</sup> radicals in the atmospheric layer near the ground. Although this rate is not sufficient to explain the complete OH discrepancy, it indicates the potentially important role of vertical transport in the lower nighttime atmosphere.

## 1 Introduction

The chemical removal of most atmospheric trace gases during daytime is dominated by reactions with OH radicals, when they are efficiently generated by photodissociation of ozone, nitrous acid, and other gases. Under these conditions, OH concentrations are usually in the range of  $(1-10) \times 10^6 \text{ cm}^{-3}$  (Ehhalt, 1999; Monks et al., 2009; Lu and Zhang, 2010). During nighttime, it is generally assumed that oxidation reactions with the nitrate radical (NO<sub>3</sub>) and ozone are more important than reactions by OH (Platt et al., 1984; Platt et al., 1988; Mihelcic et al., 1993; Geyer et al., 2003). In fact, measured OH concentrations in the night are often very small (less than a few times  $10^5 \text{ cm}^{-3}$ ) for rural conditions (Eisele et al., 1997; Holland et al., 1998, 2003; Schlosser et al., 2009; Kanaya et al., 2012). In contrast, much larger nocturnal OH concentrations on the order of  $1 \times 10^6 \text{ cm}^{-3}$  were observed in forests (Faloona et al., 2001) and polluted urban areas in Nashville (Martinez et al., 2003) and New York (Ren et al., 2003), which could not be explained by chemical models and have raised questions about the reliability of nighttime OH measurements (Mao et al., 2010). Unexplained high OH concentrations have also been observed at daytime under conditions with high volatile organic compound (VOC) reactivities and low NO concentrations (Tan et al., 2001; Lelieveld et al., 2008; Hofzumahaus et al., 2009; Lu et al., 2013, 2012; Whalley et al., 2011). As a possible explanation, it has been supposed that OH radicals are efficiently recycled from intermediate products in the oxidation of volatile organic compounds, such as isoprene, without involvement of NO, which is otherwise the main agent to regenerate OH by reaction with organic peroxy (RO<sub>2</sub>) and hydroperoxy (HO<sub>2</sub>) radicals. In the case of the isoprene oxidation, it has been shown that there are indeed unimolecular reactions of RO<sub>2</sub> that reproduce efficiently HO<sub>x</sub> (OH and HO<sub>2</sub>), but these processes can explain only part of the high OH daytime concentrations (Peeters and Müller, 2010; Crouse et al., 2011; Fuchs et al., 2013). There remains the question of whether the unexplained high OH concentrations at day- and nighttime have common causes. An opportunity to investigate this question is offered by OH measurements collected during the PRIDE-PRD2006 and CAREBEIJING2006 field campaigns that took place in summer 2006 in China. In these two field campaigns, the chemistry of the lower troposphere was studied by measurements of OH and HO<sub>2</sub>, *k*<sub>OH</sub> (OH reactivity = inverse chemical OH lifetime), trace gases, aerosols, photolysis frequencies, and meteorological parameters in order to better understand the processes controlling air pollution in the Pearl River Delta (PRD) and in the region around the capital city of Beijing. In these regions, surprisingly high OH concentrations were observed both at day and night. In previous publications (Hofzumahaus et al., 2009; Lu et al., 2012, 2013), the daytime observations of OH were analyzed and compared with model simulations. In the present work, the focus lies on the

nighttime observations. In the following, the nighttime data for HO<sub>x</sub> and *k*<sub>OH</sub> will be presented and compared with box model calculations. Discrepancies of the measured and modeled OH concentrations will be discussed, and the potential impact of chemistry as well as vertical exchange processes on the abundance of OH in the nocturnal boundary layer will be presented.

## 2 Methodology

### 2.1 Experimental

The campaign PRIDE-PRD2006 was performed in the Pearl River Delta in July 2006, and CAREBEIJING2006 took place in Beijing from mid-August to early September 2006. For each campaign, one measurement supersite was set up. In PRD, the measurement site Backgarden (BG) was located in a rural environment influenced by pollution from the megacity of Guangzhou, while the other site was in the suburban area Yufa (YF) in the vicinity of Beijing. Almost identical instrumentation was used at the two sites to characterize the processes of trace gas removal, photochemical ozone production and aerosol formation (Hofzumahaus et al., 2009; Lu et al., 2013, 2012, 2010a, b; Li et al., 2012; Lou et al., 2010; Xiao et al., 2009). Trace gases (HO<sub>x</sub>, O<sub>3</sub>, NO<sub>x</sub>, CO, C<sub>2</sub>–C<sub>12</sub> hydrocarbons, HONO), photolysis frequencies, and meteorological parameters (temperature, pressure, relative humidity) were measured.

OH and HO<sub>2</sub> concentrations were measured in both campaigns by laser-induced fluorescence (LIF) spectroscopy (Lu et al., 2012, 2013). With this technique, ambient air is sampled through an orifice by gas expansion into a low-pressure (3.5 hPa) volume. OH radicals are then detected by resonance fluorescence following electronic excitation by 308 nm UV laser radiation. Ambient HO<sub>2</sub> radicals are first converted into OH by reaction with added NO and then detected as OH. The two fluorescence cells to measure the ambient OH and HO<sub>2</sub>\* radicals were physically separated and each connected by a 3 m long vacuum line to a low-pressure pump. The accuracy of the OH and HO<sub>2</sub> measurements is estimated to be 20% (1σ). The accuracy is determined by the uncertainty of the calibrations that were performed with a photochemical radical source based on the VUV (185 nm) photolysis of water vapor in synthetic air (Holland et al., 2003). The measurement instrument has a known interference from ambient ozone in humid air, which produces an OH signal with a strength equivalent to an OH concentration of  $(6 \pm 2) \times 10^3 \text{ cm}^{-3}$  per ppb of ozone. All OH measurements presented here were corrected for the ozone interference, which had nighttime values of about  $4 \times 10^4$ – $2 \times 10^5 \text{ cm}^{-3}$ . The limit of detection (1σ) of the corrected OH measurements was in the range of  $(0.5-1) \times 10^6 \text{ cm}^{-3}$  at a time resolution of 5 min. The variability of the detection limit was

mainly caused by variations of the 308 nm laser power (10–60 mW).

As shown by Fuchs et al. (2011), the detection of HO<sub>2</sub> has an interference caused by specific RO<sub>2</sub> radicals. When ambient HO<sub>2</sub> is converted in the instrument into OH by reaction with NO, a fraction of ambient RO<sub>2</sub> is converted first to HO<sub>2</sub>, followed by HO<sub>2</sub>-to-OH conversion. The magnitude of the interference depends on the specific RO<sub>2</sub> radical. As a result, the HO<sub>2</sub> measurement yields a concentration which is denoted [HO<sub>2</sub>\*]:

$$[\text{HO}_2^*] = [\text{HO}_2] + \sum \alpha_i \times [\text{RO}_{2i}]. \quad (1)$$

Here,  $\alpha_i$  denotes the detection sensitivity of specific RO<sub>2*i*</sub> radicals relative to HO<sub>2</sub>. For the instrument configuration used in PRD and Beijing, the values were relatively small for simple alkanes (e.g., 4% for methyl peroxy radicals) and ranged between 70 and 90% for RO<sub>2</sub> from alkenes and aromatics (Fuchs et al., 2011; Lu et al., 2012). At night, additional organic peroxy radicals with a different chemical behavior can be formed, if unsaturated VOCs react with NO<sub>3</sub>. In this case, NO<sub>3</sub> (rather than OH) is added to a carbon double bond followed by addition of molecular oxygen. For the resulting nitrate–peroxy radicals, we have estimated  $\alpha_i$  values for the conditions in the HO<sub>2</sub> detection cell by means of model calculations based on the Master Chemical Mechanism (MCMv3.2; <http://mcm.leeds.ac.uk/MCM/>). Relative detection sensitivities of the NO<sub>3</sub>-initiated organic peroxy radicals are found to be generally small. For internal alkenes,  $\alpha_i$  is about 0.3%; for terminal alkenes, the value is about 1.9%. Since the internal alkenes react almost 100 times faster with NO<sub>3</sub> than terminal alkenes and the nighttime concentrations of internal alkenes were several times smaller than those of terminal alkenes (Table 1), the HO<sub>2</sub> interference from NO<sub>3</sub>-initiated RO<sub>2</sub> can be considered to be negligible in this study. The small HO<sub>2</sub> interference introduced by NO<sub>3</sub>-initiated RO<sub>2</sub> can be understood, since the corresponding alkoxy radicals from the RO<sub>2</sub> + NO reaction mainly decompose to OVOCs and NO<sub>2</sub> as products, instead of forming HO<sub>2</sub> and RONO<sub>2</sub>.

The measured HO<sub>2</sub> concentrations in this study are reported as HO<sub>2</sub><sup>\*</sup>, since speciated RO<sub>2</sub> measurements were not available for their correction. The limit of detection (1 $\sigma$ ) of the HO<sub>2</sub> measurements was in the range of (1–3)  $\times 10^6$  cm<sup>-3</sup> at a time resolution of 5 min. Note that the stated accuracy of 20% (1 $\sigma$ ) does not consider the bias by the uncorrected RO<sub>2</sub> contribution.

In both campaigns, total OH reactivity ( $k_{\text{OH}}$ ) of ambient air was measured by a combination of laser flash photolysis (LP) and LIF technique (Lou et al., 2010). Artificially high OH concentrations ( $\sim 5 \times 10^9$  cm<sup>-3</sup>) were generated by laser flash photolysis of ozone in a flow of sampled ambient air. The laser wavelength was 266 nm and the laser pulse duration was 10 ns. The following OH decay was observed in real time by the LIF technique. OH reactivities were determined as reciprocal OH lifetimes from the pseudo first-order decays

**Table 1.** Nighttime averaged values of observed trace gases, HO<sub>x</sub> radicals, and total OH reactivity before (20:00–24:00 CNST) and after (00:00–04:00 CNST) midnight at the measurement sites in Backgarden (BG) and Yufa (YF).

Parameter	Period 1 (20:00–00:00)		Period 2 (00:00–04:00)	
	BG	YF	BG	YF
O <sub>3</sub> (ppb)	25.8	28.9	7.4	14.2
NO (ppb)	0.25	0.18	4.8	1.2
NO <sub>2</sub> (ppb)	17.1	15.2	23.1	14.6
HONO (ppb)	1.2	0.9	2.0	1.0
CO (ppb)	998	712	1138	940
Ethane (ppb)	1.5	4.5	1.5	4.6
Ethene (ppb)	3.0	4.6	3.0	4.6
1,3-Butadiene (ppb)	N/A	0.2	N/A	0.2
Isoprene (ppb)	1.6	0.6	0.8	0.1
HC3 (ppb)	4.7	4.7	7.1	6.1
HC5 (ppb)	4.2	3.5	7.5	3.4
HC8 (ppb)	2.9	1.5	5.7	1.3
OLI (ppb)	0.4	0.1	0.7	0.1
OLT (ppb)	2.7	2.6	3.8	2.6
TOL (ppb)	7.0	8.4	13.0	6.2
XYL (ppb)	3.6	2.4	5.5	0.7
H <sub>2</sub> O (% abs)	3.4	2.2	3.4	2.2
OH (10 <sup>6</sup> cm <sup>-3</sup> )	1.6	1.5	0.9	1.0
$k_{\text{OH}}$ (s <sup>-1</sup> )	40.3	26.1	54.1	25.0
HO <sub>2</sub> <sup>*</sup> (10 <sup>8</sup> cm <sup>-3</sup> )	2.6	1.9	0.7	0.6
Temperature (°C)	31.1	24.0	29.8	22.3
Pressure (hPa)	1000.3	1006.0	1000.7	1006.3

of OH. The accuracy of the  $k_{\text{OH}}$  measurements was 7% plus 0.3 s<sup>-1</sup>, and the 1 $\sigma$  precision was 4–10% during the campaigns.

NO<sub>x</sub>, CO, and O<sub>3</sub> were measured by commercial instruments, i.e., a Thermo Electron Model 42CTL (photolytic converter for NO<sub>2</sub> detection), Model 48C, and Model 49C, respectively (Takegawa et al., 2006). The measurement precisions were 50 ppt (1 min) for NO, 170 ppt (1 min) for NO<sub>2</sub>, 1% for CO, and 0.3 ppb (1 min) for O<sub>3</sub>. At the BG site, a few gas canister samples were taken during the campaign and analyzed by gas chromatography (GC) in order to determine concentrations of C<sub>2</sub> species, while C<sub>3</sub>–C<sub>12</sub> non-methane hydrocarbons (NMHCs) were measured and identified by an automated gas chromatography flame ionization detector (GC-FID) system (Wang et al., 2008). At the YF site, C<sub>2</sub>–C<sub>12</sub> NMHCs were measured and identified by a GC-FID/PID (photoionization detector) instrument (Xie et al., 2008). Accuracy and detection limits of the GC measurements were 10 and 1–90 ppt, respectively. HONO was determined by a modified commercial instrument based on long-path liquid absorption photometry (LOPAP) (Li et al., 2012) with a detection limit of 7 ppt and an accuracy of 10%. Surface meteorological parameters were obtained by a Vaisala Weather Transmitter WXT520 and a R.M. Young meteorological station for BG and YF, respectively. Additionally, a 3-D-ultrasonic anemometer was deployed at both measurement

sites to determine the local wind and local turbulence. In PRD, peroxy acetic nitrate (PAN) measurements were performed with an online gas chromatography equipped with an electron capture detector (GC-ECD) technique (Wang et al., 2010). The accuracy of the PAN measurement is estimated to be 25 % by convoluting the errors of the photochemical PAN standard, variability of the calibration results, inlet and column thermal losses, etc.

A summary of the general conditions during nighttime is given in Table 1, which presents averaged values of measurements before (20:00–24:00 CNST) and after (00:00–04:00 CNST) midnight (CNST: Chinese Standard Time; i.e., UTC + 8h) for the days when HO<sub>x</sub> and NO<sub>x</sub> measurements are available. The daytime conditions have been presented in Lu et al. (2012, 2013).

## 2.2 Chemical model

A zero-dimensional chemical box model based on the Regional Atmospheric Chemical Mechanism (Stockwell et al., 1997) upgraded with the isoprene degradation scheme by Geiger et al. (2003) and Karl et al. (2006), RACM-MIM-GK, has been applied to simulate the diurnal cycles of OH, HO<sub>2</sub>, HO<sub>2</sub><sup>\*</sup>, and RO<sub>2</sub>, and *k*<sub>OH</sub> for PRIDE-PRD2006 (Lu et al., 2012) and CAREBEIJING2006 (Lu et al., 2013). In the present work, we analyze the nighttime data. The model runs are constrained by the measured time series of O<sub>3</sub>, HONO, NO, NO<sub>2</sub>, CO, VOCs, photolysis frequencies, water vapor, ambient temperature, pressure for each individual night, and assumed deposition loss of model-generated species (mimicked by a lifetime of 24 h). Beside the base model runs (denoted M0), additional sensitivity runs are performed in this work to test modified chemical mechanisms for nighttime conditions (see below).

## 3 Results

### 3.1 Nighttime observations

During the PRIDE-PRD2006 and CAREBEIJING2006 campaigns, complete sets of nighttime measurements of HO<sub>x</sub> and other trace gases were obtained on seven (9–10, 12–13, 19–20, 20–21, 21–22, 23–24, 24–25 July) and nine (18–19, 19–20, 20–21, 21–22, 22–23, 23–24, 26–27, 29–30, 30–31 August) nights, respectively. The nocturnal variations of HO<sub>x</sub>, *k*<sub>OH</sub>, NO, O<sub>3</sub>, NO<sub>2</sub>, CO, and isoprene are displayed in Figs. 1 and 2. Here, nighttime is defined to be the period when the solar zenith angle was larger than 90°. In PRD, the sunrise and sunset times were 05:57 and 19:12 CNST, respectively. In Beijing, the sunrise and sunset was at 05:42 and 18:52 CNST.

Significant amounts of nocturnal OH and HO<sub>2</sub><sup>\*</sup> were observed in both campaigns well above the detection limits of the instrument for both radical species. The half-hourly averaged OH concentrations at night were on the order of (0.5–

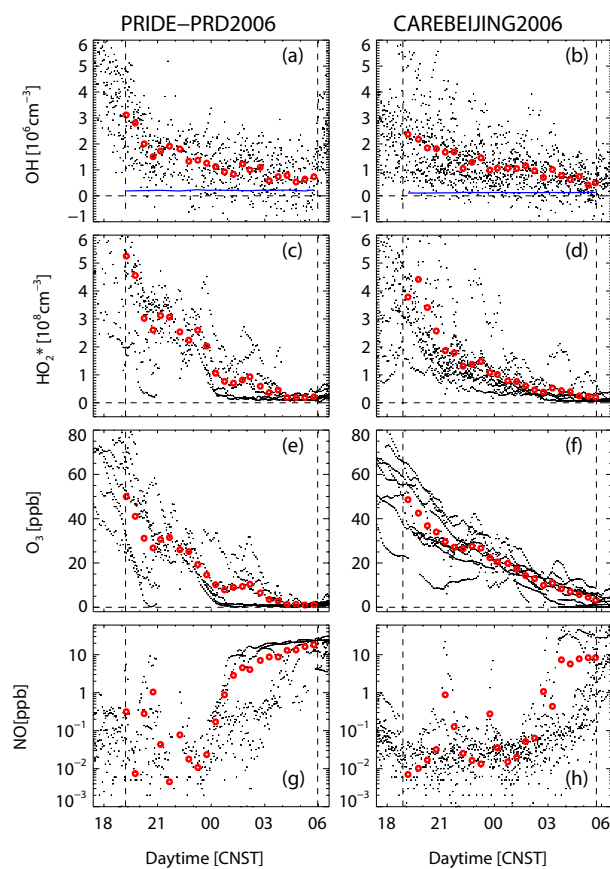


**Figure 1.** Observed concentrations of OH, HO<sub>2</sub><sup>\*</sup>, O<sub>3</sub>, and NO during nighttime PRIDE-PRD2006 and CAREBEIJING2006. The black symbols denote the original measurements; the red circles denote half-hourly averaged values. NO is displayed on a logarithmic scale. In (a) and (b), the corresponding 1σ OH detection limits (1 h) are shown as solid blue lines. The local sunset and sunrise times are marked by the dashed vertical lines.

3) × 10<sup>6</sup> cm<sup>-3</sup>, which are high values comparable to daytime observations in polluted cities (Emmerson et al., 2005) and forested areas (Whalley et al., 2011). The concentrations of HO<sub>2</sub><sup>\*</sup> were two orders of magnitude larger than those of OH, with half-hourly averaged concentrations within the range of (0.2–5) × 10<sup>8</sup> cm<sup>-3</sup>. As a general feature, the observed OH and HO<sub>2</sub><sup>\*</sup> concentrations declined gradually from high values at sunset to low values close to the limit of detection shortly before sunrise. The nighttime trend of HO<sub>x</sub> is correlated with decreasing O<sub>3</sub>, which was titrated by nocturnal NO emissions and became depleted in the late night between 03:00 and 06:00 CNST. The NO mixing ratio was generally small in the first half of the night and started – due to ongoing anthropogenic emissions – to increase rapidly by more than three orders of magnitude after midnight, when ozone became depleted. The reaction of NO with HO<sub>2</sub><sup>\*</sup> in the early morning was probably the reason for the vanishingly low HO<sub>2</sub><sup>\*</sup> concentrations at the end of the night. Diesel-powered

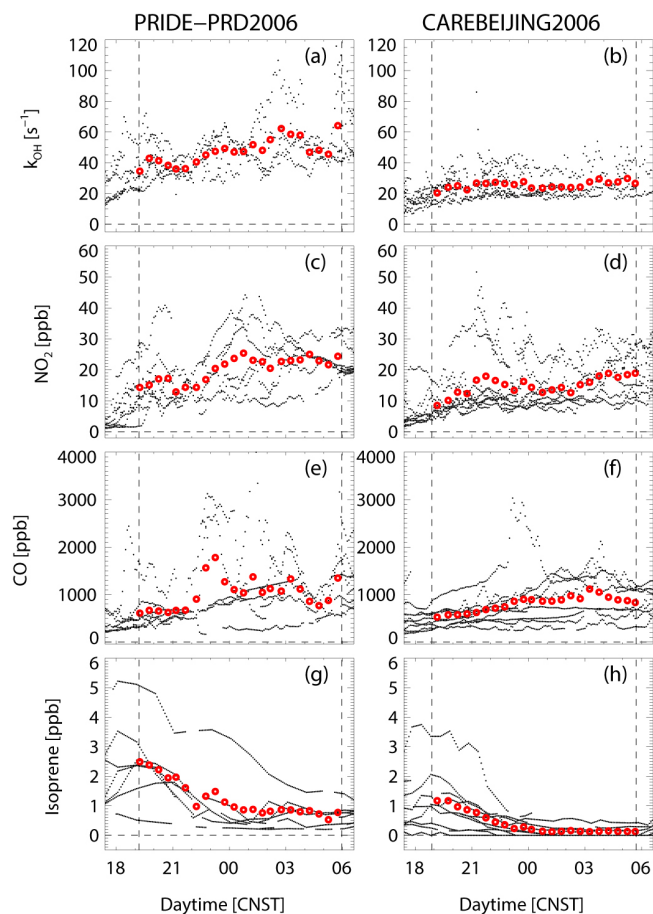


**Figure 2.** Observed values of  $k_{\text{OH}}$ ,  $\text{NO}_2$ , CO, and isoprene during PRIDE-PRD2006 and CAREBEIJING2006. The black symbols denote the original measurements, the red circles denote half-hourly averaged values for  $k_{\text{OH}}$ ,  $\text{NO}_2$ , CO, and isoprene. The local sunset and sunrise time are marked by the dashed vertical lines.

trucks and other combustion activities were the likely reason for the NO emissions in PRD (Lu et al., 2012; Garland et al., 2008). At the Yufa site, nighttime emissions came from Beijing city, the nearby highway about 1 km to the east of the measurement site, or from highly industrialized regions outside Beijing (Lu et al., 2013; Garland et al., 2009; Matsui et al., 2009). The traces of CO and isoprene showed big differences from night to night. The variabilities of the two compounds indicate the varying influence of biogenic and anthropogenic emissions sources. We analyzed the correlations between observed OH and HO<sub>2</sub><sup>\*</sup> radicals with the CO and isoprene concentrations. We found that the corresponding correlation coefficients ( $r^2$ ) are small (see Table 2) and thus do not provide a useful hint to the chemical reason of the significant high nighttime HO<sub>x</sub> concentrations. Despite the strong variability of individual trace gases, nocturnal  $k_{\text{OH}}$  was relatively constant and maintained high values between 40 and 50 s<sup>-1</sup> in PRD and 25 s<sup>-1</sup> in Yufa.

**Table 2.** Correlation coefficients ( $r^2$ ) between observed OH and HO<sub>2</sub><sup>\*</sup> radicals with the CO and isoprene concentrations in both PRD and Beijing.

	$r^2(\text{CO,OH})$	$r^2(\text{CO,HO}_2^*)$	$r^2(\text{ISO,OH})$	$r^2(\text{ISO,HO}_2^*)$
PRD	0.070	0.066	0.062	0.340
Beijing	$4 \times 10^{-6}$	0.036	0.190	0.371

### 3.2 Model and measurement intercomparisons

A box model was used to calculate concentrations of OH, HO<sub>2</sub>, HO<sub>2</sub><sup>\*</sup>, and total OH reactivities at the two measurement sites. Figure 3 compares mean nighttime profiles of the model results and observations. The averaged modeled OH concentrations lie within the range of  $(1\text{--}2) \times 10^5 \text{ cm}^{-3}$  during the whole night and are significantly smaller than the observed values. Shortly after sunset, the measurement-to-model ratio at PRD is about a factor of 10 and decreases to about 4 at the end of the night. In Yufa, the corresponding ratio changed from 20 after sunset to 2 before sunrise. For comparison, model results were also calculated based on the chemically more explicit Master Chemical Mechanism (MCMv3.2). The good agreement of the OH results from RACM-MIM-GK (M0) and MCMv3.2 demonstrates that the model deviations from the measurements are not caused by VOC lumping in the base mechanism.

In the case of HO<sub>2</sub><sup>\*</sup>, the models (RACM-MIM-GK and MCM) reproduce well the observed magnitude of concentrations and their nocturnal variabilities, especially for the PRIDE-PRD2006 campaign. HO<sub>2</sub><sup>\*</sup> contains a substantial RO<sub>2</sub> contribution, which is seen as the difference of the modeled HO<sub>2</sub><sup>\*</sup> and HO<sub>2</sub> curves in Fig. 3. The modeled nighttime HO<sub>2</sub><sup>\*</sup>-to-HO<sub>2</sub> ratio has values within the range of 1.6–4 at the PRD site, and values of 1.4–2 at Yufa. The ratios are largest after sunset when NO had low mixing ratios and decrease after midnight when NO rises and thereby influences both the amount and speciation of the interfering RO<sub>2</sub>.

The magnitude of the measured  $k_{\text{OH}}$  is reproduced well by both model mechanisms before midnight at PRD and for the whole night at Yufa (Fig. 3). For both campaigns, about half of the modeled reactivity is contributed by measured trace gases (CO, NO<sub>x</sub>, non-oxygenated VOCs) and half by model-generated oxidation products (mainly HCHO and other OVOCs). The averaged concentration level of HCHO was 10–12 ppb for PRD and 9–11 ppb for Beijing without significant variations. Though the assumed deposition lifetime has a significant influence on the modeled HCHO and OVOC concentrations, it has a relatively small impact on the simulated results of OH, HO<sub>2</sub><sup>\*</sup>, and OH reactivity, as already discussed in detail by Lou et al. (2010) and Lu et al. (2012, 2013). After midnight, the OH reactivity in PRD was about 30% larger than calculated by the model, pointing to unmeasured reactants that were likely caused by anthropogenic

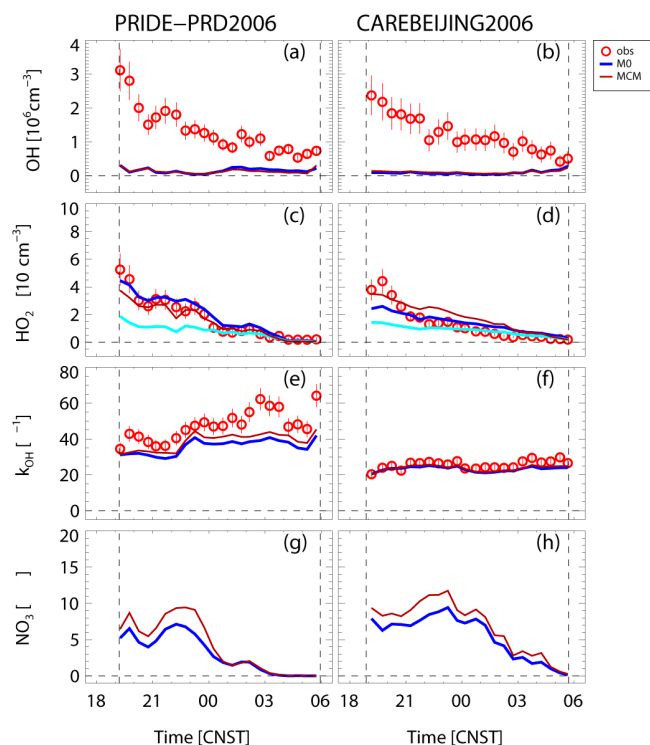


**Figure 3.** Model–measurement comparison of mean nighttime variations of OH, HO<sub>2</sub><sup>\*</sup>, and  $k_{\text{OH}}$  for PRIDE-PRD2006 and CAREBEIJING2006. The error bars attached to the observed data points denote the combined uncertainty from precision and accuracy ( $1\sigma$ ). In addition, model-simulated concentrations of HO<sub>2</sub> (M0, cyan lines in (c) and (d)) and NO<sub>3</sub> ((g) and (h)) are shown.

emissions or to oxidation products underestimated by the model. The largest model–measurement discrepancies of  $k_{\text{OH}}$  appeared in the nights of 23–24 and 24–25 July (Lou et al., 2010), probably caused by smoldering biomass fires as indicated by the analysis of measured aerosols (Garland et al., 2008). More than 70 % of the total OH reactivity at both measurement sites was caused by VOCs (Lou et al., 2010; Lu et al., 2012, 2013). It should be noted that the VOC speciation at both sites differed considerably between day and night. While isoprene had the largest reactivity among the measured hydrocarbons at daytime (70 % at PRD; 32 % at Yufa), its contribution was small at night (7–16 % at PRD; 3–7 % at Yufa). Instead, simple alkenes (e.g., propene, butenes) and aromatic compounds (e.g., toluene, xylenes) dominated the reactivities of measured VOCs at night at both measurement sites.

Nitrate radicals that are formed by reaction of NO<sub>2</sub> and O<sub>3</sub> can be an important oxidant at night, when their photolysis is negligibly small. For both campaigns, modeled nighttime concentrations of NO<sub>3</sub> are predicted to be largest (5–10 ppt) in the first half of the night. After midnight, when the mixing ratio of NO starts to rise, a decrease of NO<sub>3</sub> is predicted as a result of its fast reaction with NO (Fig. 3). Of the averaged

nighttime profiles, the modeled NO<sub>3</sub> looks to be significant for periods in which the NO is large (e.g., >10 ppbv after midnight). This is a consequence of averaging some nights with lower NO and non-zero NO<sub>3</sub> together with others that have higher NO and zero NO<sub>3</sub>.

The total amount of modeled nighttime peroxy radicals (RO<sub>2</sub> + HO<sub>2</sub>) and their speciation is displayed in Fig. 4a, c. The total concentration is largest before midnight, when NO was small, and decreases after midnight due to the reaction of the peroxy radicals with increasing NO. Unlike at daytime (Fig. 4b, d), when HO<sub>2</sub>, methyl peroxy (MO<sub>2</sub>), and isoprene peroxy (ISOP) radicals were the dominating species, peroxy radicals at night are predicted to be mostly  $\beta$ -nitrate alkylperoxy radicals (OLNN and OLND) resulting from addition reactions of NO<sub>3</sub> to alkenes. In the RACM mechanism, OLNN denotes peroxy radicals which upon reaction with NO form HO<sub>2</sub>, organic nitrates, and NO<sub>2</sub>, whereas OLND decompose upon reaction with NO and yield carbonyl compounds and NO<sub>2</sub> without formation of HO<sub>2</sub>.

### 3.3 Nighttime oxidation rates

The measured nocturnal OH concentrations in PRD and Yufa are unexpectedly large (see Sect. 3.2). In the presence of high OH reactivities as found in the night, they imply large OH turnover rates given by the product  $k_{\text{OH}} \times [\text{OH}]$  (Fig. 5). On average, the OH turnover rates are on the order of 8.5 ppb h<sup>-1</sup> and 3.8 ppb h<sup>-1</sup> in PRD and Yufa, respectively, with equally large oxidation rates of the sum of reactive trace gases (e.g., VOC, CO, NO<sub>2</sub>) reacting with OH. At daytime, oxidation rates reached maximum values of about 40 and 25 ppb h<sup>-1</sup>, respectively. As a result, nocturnal OH would be responsible for about a quarter of the total trace gas oxidation by OH integrated over 24 h for the air masses characterized at the measurement sites. It should be noted that the observed high nighttime OH may be confined to a shallow layer near the surface where the measurements took place (see Sect. 4.4.2). Thus, the general relevance of nighttime compared to daytime oxidation by OH in the lower troposphere cannot be derived from our data.

The nocturnal VOC oxidation rates by OH (6.8 and 2.6 ppb h<sup>-1</sup> in PRD and Yufa, respectively) are significantly larger than the estimated VOC reaction rates with NO<sub>3</sub>, which were calculated by the base model to be around 0.6 and 0.3 ppb h<sup>-1</sup> for PRD and Beijing, respectively (Fig. 5). They represent upper limits, since the model includes only homogeneous gas-phase reactions and neglects the possible heterogeneous loss of NO<sub>3</sub> as well as of the major reservoir species N<sub>2</sub>O<sub>5</sub> (e.g., Brown et al., 2006). Additionally, the nighttime ozonolysis rates were calculated to be around 0.3 and 0.1 ppb h<sup>-1</sup> for PRD and Beijing, respectively, which are even smaller than for NO<sub>3</sub>. Clearly, the VOC oxidation by OH appears to dominate over the VOC degradation by NO<sub>3</sub> and O<sub>3</sub> (Fig. 5), in contrast to the general view that nighttime OH should play only a minor role (e.g., Geyer et al., 2003;

**Table 3.** Overview of mean nighttime OH concentrations, observed-to-modeled OH ratios (OH<sub>obs</sub>/OH<sub>mod</sub>) and limit of OH detection (LOD) from our studies and from other field campaigns where higher-than-expected nighttime OH concentrations were reported.

Field campaign	Environment	OH [cm <sup>-3</sup> ]	OH <sub>obs</sub> /OH <sub>mod</sub>	LOD [cm <sup>-3</sup> ]	References
PROPHET <sup>a</sup>	Forest	1.1 × 10 <sup>6</sup>	46	0.05 × 10 <sup>6</sup> (0.5 h)	Faloona et al. (2001)
SOS-Nashville <sup>a</sup>	Urban	0.8 × 10 <sup>6</sup>	> 10	0.8 × 10 <sup>6</sup> (1 min)	Martinez et al. (2003)
PMTACS <sup>a</sup>	Urban	1.0 × 10 <sup>6b</sup>	9 <sup>b</sup>	0.3 × 10 <sup>6</sup> (1 min)	Ren et al. (2003a, b)
MCMA <sup>a</sup>	Urban	0.6 × 10 <sup>6b</sup>	1.5 <sup>b</sup>	0.2 × 10 <sup>6</sup> (1 min)	Shirley et al. (2006)
TORCH	Urban	0.3 × 10 <sup>6</sup>	2	0.03 × 10 <sup>6</sup> (15 min)	Emmerson and Carslaw (2009)
IMPACT-L	Urban	0.4 × 10 <sup>6</sup>	4	0.13 × 10 <sup>6</sup> (10 min)	Kanaya et al. (2007)
PRIDE-PRD	Rural <sup>c</sup>	1.3 × 10 <sup>6</sup>	11	0.14 × 10 <sup>6</sup> (1 h)	This study
CAREBEIJING	Suburban	1.2 × 10 <sup>6</sup>	18	0.14 × 10 <sup>6</sup> (1 h)	This study

<sup>a</sup> The Penn State LIF instrument was used for OH measurement. It is possible that the reported nighttime data are enhanced by an artifact as reported by Mao et al. (2012).

<sup>b</sup> The concentrations are scaled up by a factor of 1.44 herein according to Mao et al. (2010).

<sup>c</sup> Strongly urban influenced.

Sadanaga et al., 2003; Monks et al., 2009; Finlayson-Pitts and Pitts Jr., 2000).

## 4 Discussion

### 4.1 Unexpectedly large nighttime OH concentrations

The comparison of the measured and modeled OH concentrations over averaged nighttime profiles in Fig. 3 shows that the observed magnitude of the nocturnal OH is unexpectedly large. We also performed a correlation analysis between observed and modeled radical concentrations for each night. The squared correlation coefficients between observed and modeled OH radicals were lower than 0.07 for each night in both campaigns. The slopes of the linear regression between modeled and observed OH radicals was between 0.1 and 4 % for individual nights in PRD and between 0.1 and 8 % in Beijing. These correlations agree well with the behavior of the averaged data of observation and modeling, so the following discussion will use the averaged nighttime profiles.

The discrepancy of up to an order of magnitude is significant since it is much larger than the measurement and model errors. In the past, higher-than-expected nighttime OH concentrations were reported also in other studies (Table 3). The sites where the measured OH exceeded the model-predicted concentrations were located in forests (Faloona et al., 2001) and urban areas (Martinez et al., 2003; Ren et al., 2003a, b; Shirley et al., 2006; Emmerson and Carslaw, 2009; Kanaya et al., 2007). The reported concentrations in these studies have similar nighttime values of (0.5–1) × 10<sup>6</sup> cm<sup>-3</sup>, but deviate by different factors (2–46) from the model predictions. The level of nighttime OH and the model underprediction in the present work fall into the range of the other studies. All studies have in common that the OH reactivity was high, with values larger than 10 s<sup>-1</sup> (Lou et al., 2010, and references therein).

The model–measurement discrepancies may be due to deficiencies in the models. Thus, previous studies discussed different possibilities for missing nighttime sources of OH. For example, ozonolysis of reactive biogenic hydrocarbons as a radical source (Faloona et al., 2001), vertical transport of radical precursors and their thermal decomposition (Geyer and Stutz, 2004), or enhanced OH regeneration from the reaction of peroxy radicals with reactants other than NO (Faloona et al., 2001; Martinez et al., 2003) was investigated. However, no conclusive explanation for the observed elevated nighttime OH has been found. This has raised the question of whether the unexplained high OH observations at night could be caused by measurement artifacts. For the Penn State LIF instrument (used in Faloona et al., 2001; Martinez et al., 2003; Ren et al., 2003a, b; Shirley et al., 2006), extensive instrumental tests were performed ruling out a number of suspected potential interferences. For example, it was shown that spectral interferences from SO<sub>2</sub> and HCHO during the laser excitation of OH at 308 nm and artificial production of OH in the instrument by laser photolysis of ozone or HONO can be neglected (Ren et al., 2004). Recently, the Penn State group reported a measurement artifact in their instrument that they discovered during field measurements in a pine forest (Mao et al., 2012). OH measurements using the traditional spectral modulation of the OH resonance fluorescence at 308 nm were compared to a new chemical modulation technique that uses C<sub>3</sub>F<sub>6</sub> for OH quenching in ambient air samples. About half of the measured OH at day and night in the forest could be identified as an artifact that produced OH inside the instrument. The artifact increases with temperature and is possibly the result of the decomposition of biogenic VOC reaction products, such as Criegee biradicals from the ozonolysis of alkenes (Mao et al., 2012). Thus, it could have been a significant contributor to previous nighttime OH measurements in high VOC environments. Since other LIF instruments (including the one in this work) also use spectral modulation of the 308 nm OH fluorescence

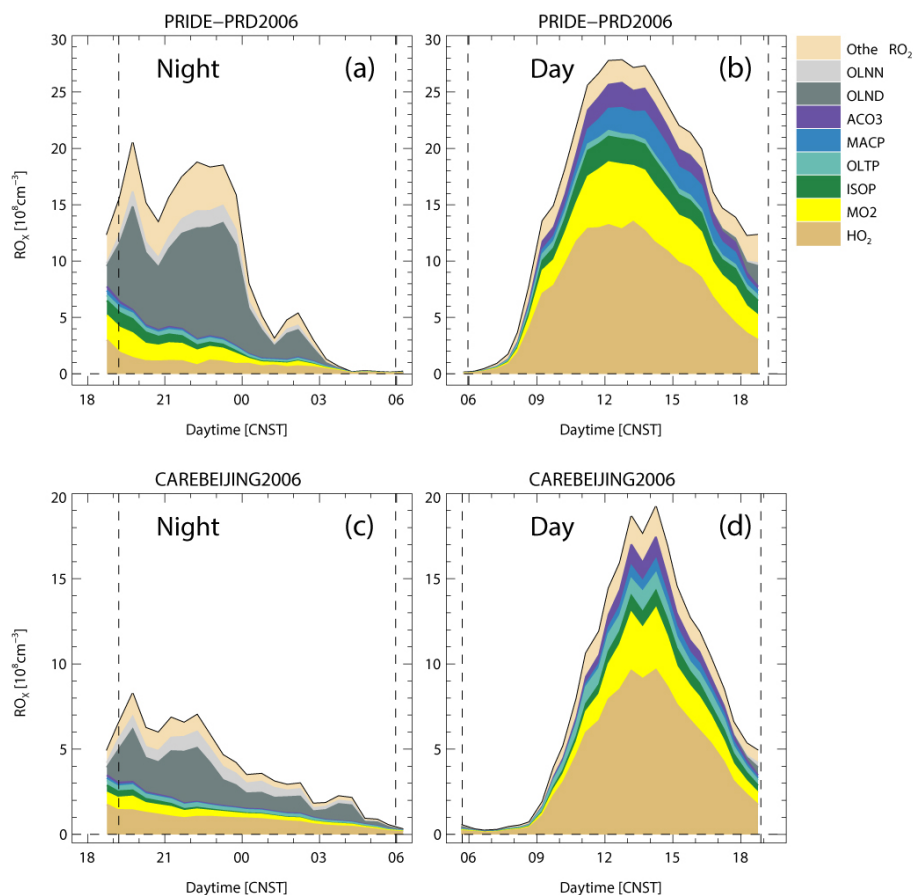


**Figure 4.** Modeled (M0) peroxy radical (= RO<sub>2</sub> + HO<sub>2</sub>) concentrations and their speciation at night (left panels) and during daytime (right panels).

signal, they might also be affected by the artifact. The sensitivity to the interference is expected to depend on the instrumental design, which differs from instrument to instrument, for example, in terms of the gas inlet, the gas-flow residence time in the instrument, the geometry of the detection cell, or cell pressure (Mao et al., 2012). Therefore, it is a priori not clear whether other OH LIF instruments are significantly affected by the problem.

In other campaigns, the LIF technique used in this work has never shown such high nighttime OH concentrations as reported here. Previous nighttime measurements showed concentrations well below the detection limit of typically  $(3\text{--}5) \times 10^5 \text{ cm}^{-3}$  at 1–2 min time resolution. When the data were averaged over longer time spans, concentrations were found to be on the order of  $1 \times 10^5 \text{ cm}^{-3}$  or smaller. For example, OH concentrations of  $(3 \pm 6) \times 10^4 \text{ cm}^{-3}$  (1 h average) were reported for the POPCORN campaign in a rural environment in northeastern Germany (Holland et al., 1998). During the BERLIOZ campaign, a mean nighttime concentration of  $(4 \pm 1) \times 10^4 \text{ cm}^{-3}$  (campaign average) was determined in a rural–urban transition region near the city of Berlin (Holland et al., 2003) in good agreement with model

predictions (Geyer et al., 2003). In the latter campaign, slightly higher OH concentrations of  $(1.8 \pm 0.8) \times 10^5 \text{ cm}^{-3}$  were observed in one night for which the model predicted  $(4 \pm 0.7) \times 10^5 \text{ cm}^{-3}$  (Geyer et al., 2003).

The LIF technique used in the present work was tested in several OH intercomparisons with respect to its calibration and possible interferences. The majority of data of the comparisons was collected under daytime conditions. There was good agreement typically within 20 % with an independent OH reference instrument based on folded long-path differential optical absorption spectroscopy (DOAS, Forschungszentrum Jülich) in the POPCORN field campaign (Hofzumahaus et al., 1998), as well as in the atmosphere simulation chamber SAPHIR in Jülich (Schlosser et al., 2007, 2009). The international comparison HO<sub>x</sub>Comp 2006 offered the opportunity to compare our LIF instrument for day- and nighttime conditions with a chemical ionization mass spectrometer (CIMS; German Weather Service) that uses a completely different OH detection principle. The field measurements took place on the campus of Forschungszentrum Jülich, which is located in a mixed deciduous forest (Schlosser et al., 2009). The data showed an OH calibration difference of a factor



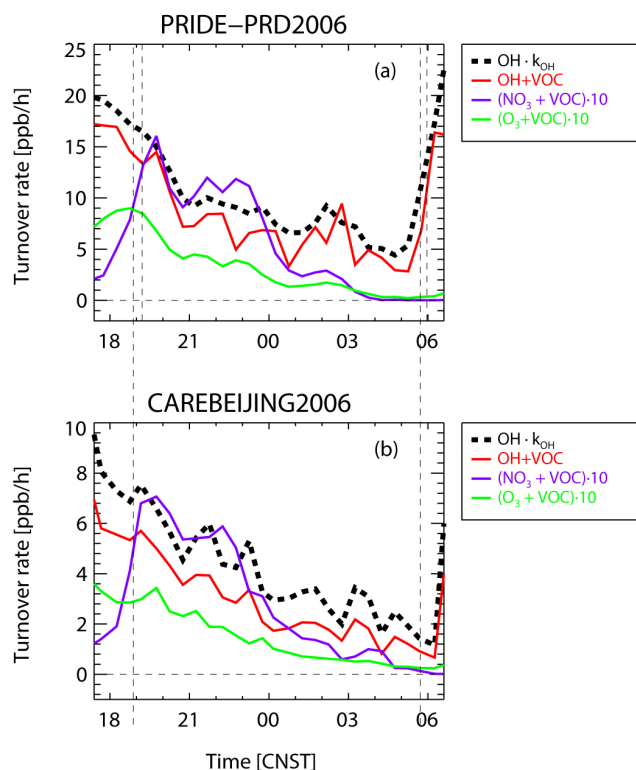


**Figure 5.** Nighttime oxidation rates of VOCs (i.e., observed HCs + modeled OVOCs) for their reaction with OH, NO<sub>3</sub>, and O<sub>3</sub> during PRIDE-PRD2006 and CAREBEIJING. The VOC oxidation rate for OH was estimated as the difference of the measured total OH reaction rate ( $k_{\text{OH}} \times [\text{OH}]$ , black dashed line) and the calculated reaction rates of OH with CO and NO<sub>x</sub>. The reaction rates of NO<sub>3</sub> and O<sub>3</sub> are taken from the base model and use modeled NO<sub>3</sub> and measured O<sub>3</sub> concentrations, respectively. The vertical dashed lines denote the sunset and sunrise.

of 1.4, which could be explained by the calibration uncertainties of LIF (20 %) and CIMS (38 %). Only a very small, insignificant offset of  $(0.04 \pm 0.03) \times 10^6 \text{ cm}^{-3}$  was found in the linear regression of the two instruments. The CIMS technique discriminates between OH and Criegee radicals by chemical modulation, and its OH data are therefore expected to be free from interferences by Criegee radicals. Thus, the small offset in the regression between LIF and CIMS indicates that the LIF measurements were likely not subject to an artifact as is discussed by Mao et al. (2012). More recently, new measurement comparisons were performed between LIF and DOAS (both Forschungszentrum Jülich) in SAPHIR under daytime conditions simulating the air composition encountered during PRIDE-PRD2006 and CAREBEIJING2006. For high VOC reactivities up to  $30 \text{ s}^{-1}$  and low NO concentrations (0.1–0.3 ppb), good agreement between LIF and DOAS was obtained. Here, the regression analysis gave a small, significant offset of  $(1.0 \pm 0.3) \times 10^5 \text{ cm}^{-3}$  (Fuchs et al., 2012). None of the abovementioned tests provides a direct indication of artifacts that would explain the

magnitude of the nighttime OH data in PRD and Yufa. There is the possibility that our tests have missed interferences that were present in PRD and Yufa at night, but not during the abovementioned OH intercomparisons. For that reason, further field and laboratory measurements are planned, for example under consideration of the chemical modulation technique suggested by Mao et al. (2012).

Faloona et al. (2001) found measured nocturnal isoprene decays in a forest to be consistent with their nighttime measurements of OH. If we assume that isoprene at the measurement sites in PRD and Yufa was produced and advected from biogenic emission sources during daylight and its leftover after sunset was predominantly removed by reaction with OH, the nocturnal isoprene decays in PRD and Yufa would indicate OH concentrations of about  $1 \times 10^6 \text{ cm}^{-3}$ . However, such an estimate has large uncertainties that are difficult to quantify. Besides its chemical removal by OH, isoprene is also subject to transport, for which we have insufficient knowledge with respect to the spatial/vertical isoprene distribution around the measurement sites. As diagnosed by Sillman et al. (2002) for the Michigan forested areas, the nighttime loss of isoprene can be attributed to three factors: chemical reaction with OH, vertical diffusion, and advection. In their model results, the observed loss of isoprene was mainly caused by the vertical diffusions. Nevertheless, Sillman et al. (2002) also pointed out that in a shallow layer near the surface, the chemical reaction with OH might be important as diagnosed by Faloona et al. (2001) for the same campaign. Furthermore, in the shallow nocturnal boundary layer, weak isoprene emitters could still play a role, such as emissions from urban traffic (Lee and Wang, 2006; Liu et al., 2008) and biogenic emissions under dark conditions, which are usually neglected compared to daytime emissions (Guenther, 1999; Shao et al., 2001). Therefore, further in-depth OH estimates from nocturnal isoprene observations appear not to be meaningful.

#### 4.2 Missing nighttime OH source

On the assumption that the nighttime OH is in steady state, a missing nocturnal OH source ( $P(\text{OH})_{\text{M}}$ ) can be calculated for PRD and Yufa from the difference between the known OH loss and production rates.

$$P(\text{OH})_{\text{M}} = k_{\text{OH}}[\text{OH}] - k_{\text{HO}_2+\text{NO}}[\text{HO}_2][\text{NO}] - p_{\text{OH}} \quad (2)$$

The known OH production includes the reaction of HO<sub>2</sub> with NO and the primary OH production ( $p_{\text{OH}}$ ) from the ozonolysis of alkenes. Here, as an approximation, measured HO<sub>2</sub>\* is used for HO<sub>2</sub> in Eq. (2). In general, the OH production by ozonolysis of alkenes, calculated from measured O<sub>3</sub> and alkene concentrations, was small and roughly an order of magnitude lower than the total OH loss rate. The uncertainty of the calculated  $P(\text{OH})_{\text{M}}$  is thus mainly determined by the uncertainty of observed OH,  $k_{\text{OH}}$ , NO, and HO<sub>2</sub> including its measurement interference. The mean value of the missing

**Table 4.** Radical sources and sinks calculated by the base model for the time before (20:00–24:00 CNST) and after (00:00–04:00 CNST) midnight at the measurement sites in Backgarden (BG) and Yufa (YF).

Parameter	Period 1 (20:00–00:00)		Period 2 (00:00–04:00)	
	BG	YF	BG	YF
Primary RO <sub>x</sub> sources (ppb h <sup>-1</sup> )	1.03	0.47	0.34	0.17
O <sub>3</sub> + alkenes	43 %	44 %	49 %	46 %
NO <sub>3</sub> + VOC	57 %	56 %	51 %	54 %
HO <sub>2</sub> → OH conversion (ppb h <sup>-1</sup> )	0.40	0.21	0.99	0.23
HO <sub>2</sub> + NO	92 %	83 %	99 %	94 %
Total OH reactivity (s <sup>-1</sup> )	33	24	39	22
OH + NO <sub>x</sub>	10 %	14 %	14 %	15 %
OH + CO	17 %	17 %	17 %	25 %
OH + VOC*	73 %	69 %	69 %	60 %
OH + Isoprene	12 %	6 %	5 %	2 %

\* The VOC contribution includes isoprene, which is listed separately in the line below.

nocturnal OH source is calculated to be about  $7.0 \pm 1.8$  and  $3.3 \pm 0.8$  ppb h<sup>-1</sup> for PRD and Beijing, respectively. These values are much smaller than the missing OH sources of 25 and 11 ppb h<sup>-1</sup>, respectively, required to explain the daytime OH observations at the same measurement sites (Lu et al., 2012, 2013).

### 4.3 Production and loss of RO<sub>x</sub>

The strength of the missing OH source is considerably larger than the production rate of RO<sub>x</sub> (the sum of OH, HO<sub>2</sub>, and RO<sub>2</sub>) estimated by the base model (cf. Table 4). In PRD, the primary nocturnal RO<sub>x</sub> production is calculated to be about 0.3–1 ppb h<sup>-1</sup> dominated by ozonolysis and NO<sub>3</sub> oxidation of VOC, with comparable contributions from O<sub>3</sub> and NO<sub>3</sub> reactions. Only 20 % of this production gives directly OH. Secondary OH formation dominated by conversion of HO<sub>2</sub> with NO exceeds the primary OH formation during the whole night over a large range of NO mixing ratios (cf. Fig. 1). The modeled OH reactivity is dominated by VOC (60–70 %) of which isoprene contributed only 6–12 %. For Beijing, the base model predicts similar relative strengths of the OH sources and sinks as in PRD, but the absolute values of the calculated reaction rates are roughly a factor of 2 smaller than in PRD. Interestingly, the factor of 2 also applies to the missing OH sources determined for both measurement sites (see above).

A more detailed view of the modeled reaction rates controlling RO<sub>x</sub> in PRD and Yufa is presented in Figs. 6–9. For each site, the situation before and after midnight is shown. The figures display the total primary production rates, the radical-to-radical conversion rates, and the rates of destruction reactions which terminate the radical cycling. Compared to the daytime chemistry, the nighttime chemistry is expected to be much slower. For example, the calculated rates for

the removal of OH, the HO<sub>2</sub>-to-OH conversion, or the primary OH production are about an order of magnitude smaller than at daytime (cf. Hofzumahaus et al., 2009; Lu et al., 2012, 2013). Thus, an additional process which would have a small impact during daytime could make a large change in nighttime OH. Noticeably, the turnover rates describing the thermal equilibria between organic peroxyacetyl radicals (RCO<sub>3</sub>) and peroxyacetyl nitrates (PANs), and between HO<sub>2</sub> and peroxy nitric acid (HNO<sub>4</sub>) are outstandingly large. For example, the rates are 1–2 orders of magnitude larger than those of the cycling between OH, HO<sub>2</sub>, and RO<sub>2</sub> in PRD before midnight. Thus, a small imbalance in the equilibrium could have a significant impact on the nocturnal radical concentrations. This possibility will be discussed further below (Sect. 4.4.2).

### 4.4 Potential mechanisms for additional radical production

The general features of the model–measurement comparison of OH and HO<sub>2</sub><sup>\*</sup> during nighttime – namely, the serious underestimation of the observed OH and the well-reproduced HO<sub>2</sub><sup>\*</sup> – are quite comparable to the corresponding results analyzed for daytime in both PRD (Hofzumahaus et al., 2009; Lu et al., 2012) and Beijing (Lu et al., 2013). This similarity suggests there could be an unified unknown chemical mechanism which resolves the mismatch of the current models for both the daytime and the nighttime chemistry. Therefore, the candidate mechanisms examined for the daytime chemistry are further tested herein.

The measured daytime concentrations of OH and HO<sub>2</sub><sup>\*</sup> in PRD could be well described when additional recycling Reactions (R1) and (R2) were introduced into the RACM-MIM-GK mechanism (Hofzumahaus et al., 2009; Lu et al., 2012).



If the rate constants for the hypothetical reactant X are assumed to be the same as for NO, a constant amount of 0.8 ppb was able to explain the missing OH daytime source. The application of a similar amount (1 ppb X) at night yields a significant increase of the simulated OH concentration compared to the measured values (Fig. 10). The modeled OH reaches 24–40 % of the measured concentrations and the modeled  $k_{\text{OH}}$  shows improved agreement. The agreement for HO<sub>2</sub><sup>\*</sup>, however, becomes slightly worse. A further increase of the modeled OH by raising the concentration of X even higher is limited by the growing depletion of RO<sub>2</sub> and HO<sub>2</sub>. Thus, OH, HO<sub>2</sub>, and  $k_{\text{OH}}$  cannot be matched simultaneously within their experimental uncertainties just by enhanced recycling. Further improvement can be obtained if an additional primary RO<sub>x</sub> source of 1 ppb h<sup>-1</sup> complements the additional recycling mechanism (X = 1 ppb). In this case, the

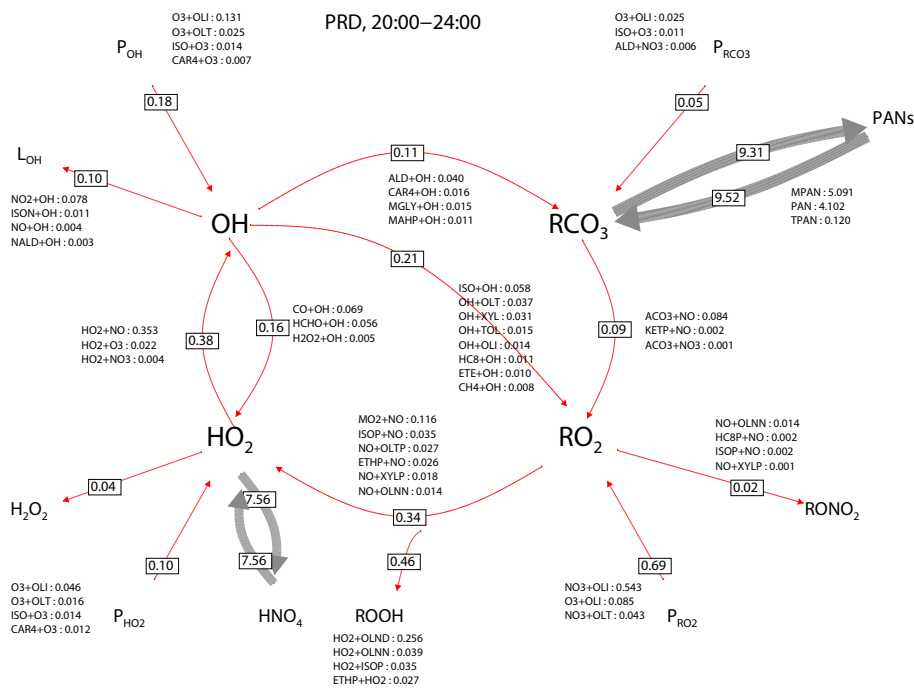


**Figure 6.** Mean RO<sub>x</sub> production, conversion, and destruction rates calculated by the base model (M0) for PRIDE-PRD2006 conditions during 20:00–24:00 CNST. The thickness of the arrows represents the relative magnitude of the reaction rates given in ppb h<sup>-1</sup>.

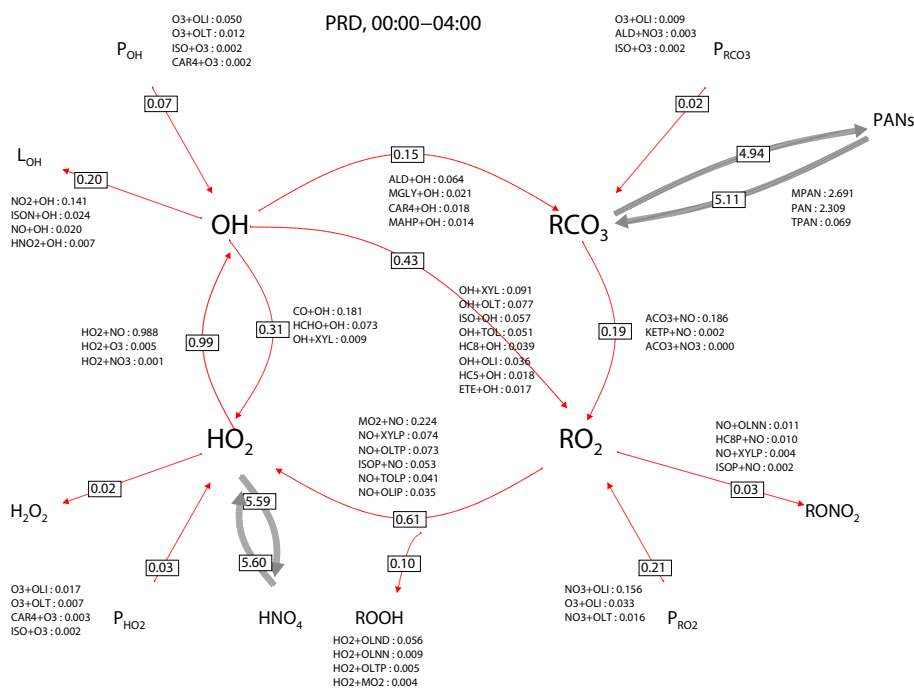


**Figure 7.** Mean RO<sub>x</sub> production, conversion, and destruction rates calculated by the base model (M0) for PRIDE-PRD2006 conditions during 00:00–04:00 CNST. The thickness of the arrows represents the relative magnitude of the reaction rates given in ppb h<sup>-1</sup>.

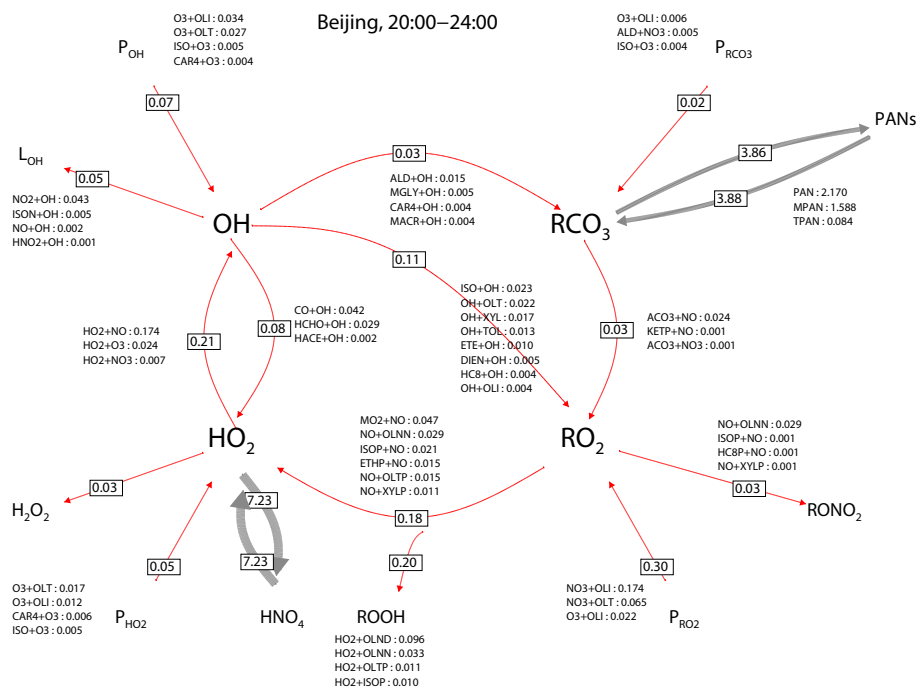


**Figure 8.** Mean RO<sub>x</sub> production, conversion, and destruction rates calculated by the base model (M0) for CAREBEIJING2006 conditions during 20:00–24:00 CNST. The thickness of the arrows represents the relative magnitude of the reaction rates given in ppb h<sup>-1</sup>.

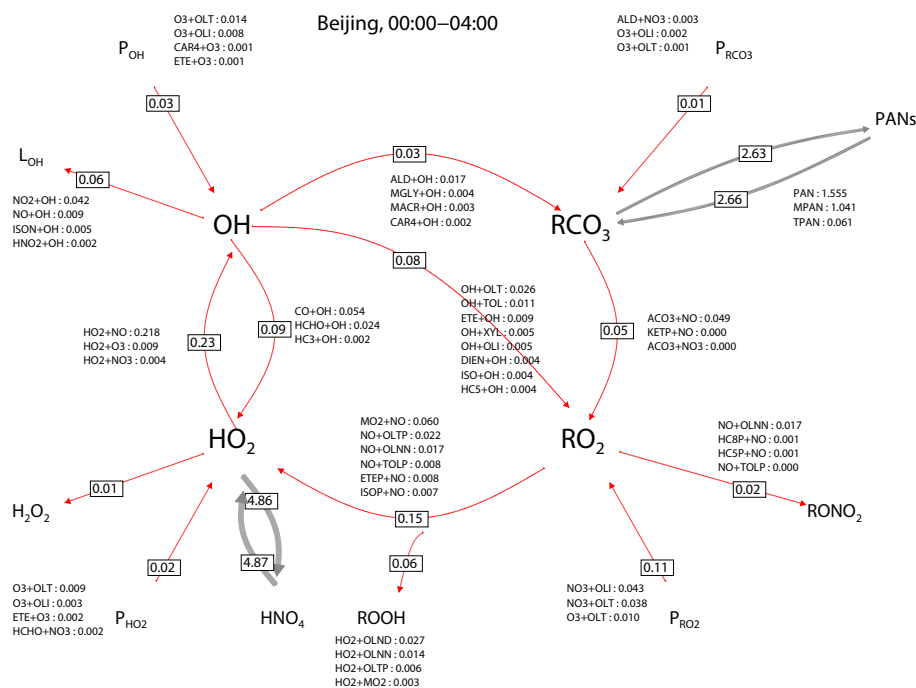


**Figure 9.** Mean RO<sub>x</sub> production, conversion, and destruction rates calculated by the base model (M0) for CAREBEIJING2006 conditions during 00:00–04:00 CNST. The thickness of the arrows represents the relative magnitude of the reaction rates given in ppb h<sup>-1</sup>.

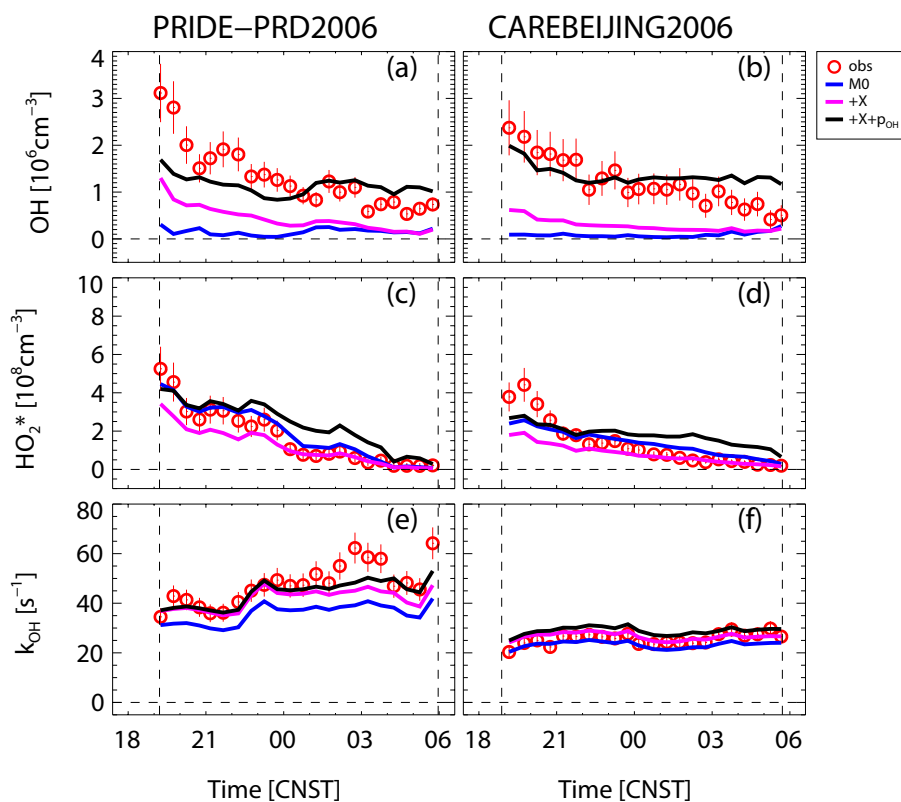


**Figure 10.** Model–measurement comparison of mean nighttime variations of OH, HO<sub>2</sub><sup>\*</sup>, and *k*<sub>OH</sub> for PRIDE-PRD2006 and CAREBEIJING2006. The model runs M0+X+*p*<sub>OH</sub> and M0+X assume additional radical recycling by X and are calculated with and without extra primary OH production (*p*<sub>OH</sub> = 1 ppb h<sup>−1</sup>), respectively. For comparison, observational and base model (M0) data from Fig. 3 are shown. Error bars attached to the observed data points denote the combined uncertainty from precision and accuracy (1σ).

modeled OH is raised to the level of the observations, but the relative nocturnal variation is not fully captured (Fig. 10). However, reasonable agreement is maintained for HO<sub>2</sub><sup>\*</sup> and *k*<sub>OH</sub>, with a tendency to overpredict HO<sub>2</sub><sup>\*</sup> at higher NO mixing ratios after midnight. Without additional recycling by X, application of an additional primary OH source in the model is not sufficient to explain the observations of OH and HO<sub>2</sub><sup>\*</sup>. A primary OH source can be tuned to match the OH observations, but would lead to a large overprediction of HO<sub>2</sub><sup>\*</sup> resulting from the enhanced rates of the reactions of OH with CO and VOC.

The situation in CAREBEIJING2006 is similar to the one in PRD. Again, only a combination of an additional primary RO<sub>x</sub> source of 1 ppb h<sup>−1</sup> and additional recycling by 1 ppb X gives a relatively good reproduction of the measured OH, HO<sub>2</sub><sup>\*</sup>, and *k*<sub>OH</sub> (Fig. 10). For both measurement sites (PRD and Yufa), the required additional primary RO<sub>x</sub> source can be implemented in the model as a source of OH, HO<sub>2</sub>, or RO<sub>2</sub>, or a combination of RO<sub>x</sub> species, all yielding essentially the same model results. The reason is that the additional input of radicals is quickly redistributed among the RO<sub>x</sub> species by the recycling reactions.

Though the base (M0) and modified (M0+X+*p*<sub>OH</sub>) models yield similar nighttime results for HO<sub>2</sub><sup>\*</sup>, the predicted abundances and speciation of the peroxy radicals (RO<sub>2</sub> and HO<sub>2</sub>) are significantly different (see Figs. 4 and 11, respectively). In the base model, a large fraction of RO<sub>2</sub> (OLNN and OLND) is produced by reactions of NO<sub>3</sub> with VOC, whereas in the modified model, production of RO<sub>2</sub> is dominated by OH and destruction of RO<sub>2</sub> is enhanced by X. Nevertheless, the introduced additional pathways in M0+X+*p*<sub>OH</sub> that change the RO<sub>x</sub> budget significantly do not show an impact on the NO<sub>3</sub> budget since the simulated NO<sub>3</sub> concentration in the two model runs (M0 and M0+X+*p*<sub>OH</sub>) were almost identical. For the VOC in PRD and Yufa, the HO<sub>2</sub> measurement interference is very different for RO<sub>2</sub> species from OH and NO<sub>3</sub> reactions (see Sect. 2.1). This behavior and the different RO<sub>2</sub> composition lead accidentally to the similarity of the HO<sub>2</sub><sup>\*</sup> concentrations in the two different model scenarios.

A new radical recycling mechanism for the oxidation of isoprene by OH has been proposed theoretically to explain the unexpected high OH concentrations observed at daytime in isoprene-rich environments (Peeters et al., 2009). The corresponding Leuven isoprene mechanism (LIM) proposes two

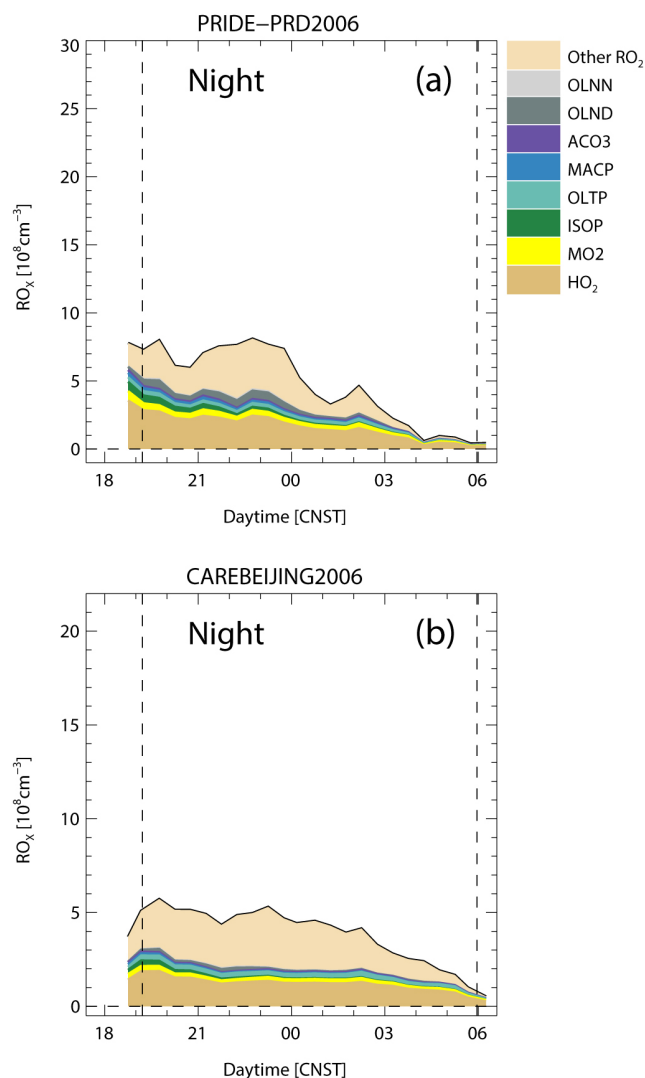


**Figure 11.** Modeled ( $M0+X+p_{OH}$ ) peroxy radical ( $= RO_2 + HO_2$ ) concentrations and their speciation at night.

isomerization reactions of isoprene peroxy radicals each followed by reproduction of HO<sub>x</sub> radicals without involvement of NO. One of the decomposition reactions gives hydroxy peroxy aldehydes as a co-product that can undergo photolysis and yield even more HO<sub>x</sub>. In the present work, the potential of LIM to provide additional nighttime OH was tested. It turns out to be ineffective for two reasons. First, the nocturnal isoprene mixing ratio was relatively small in PRD and Beijing, and secondly the photolysis of hydroxy peroxy aldehydes is missing in the night. Moreover, two recent experimental studies have demonstrated that the isomerization rates of the isoprene peroxy radicals implemented in LIM are largely overestimated (Crounse et al., 2011; Fuchs et al., 2013). Thus, isoprene is not a likely contributor to the enhanced nighttime OH concentrations in PRD and Beijing. However, the isomerization of isoprene peroxy radicals is

an example for a new type of RO<sub>2</sub> reactions that regenerate OH via isomerization without involvement of NO. Given the large concentrations of other nighttime RO<sub>2</sub> (see Fig. 4), it appears desirable in future research to further investigate the potential of other RO<sub>2</sub> species for HO<sub>x</sub> regeneration.

#### 4.4.1 Primary radical sources

The required additional RO<sub>x</sub> source of  $1 \text{ ppb h}^{-1}$  is of similar magnitude as the known source strength of VOC reactions with ozone and NO<sub>3</sub> in PRD and Beijing before midnight (cf. Table 4). Yet, it is difficult to find an obvious explanation for an increase of the primary RO<sub>x</sub> production rate by a factor of 2 or more. One possible reason could be the reaction of O<sub>3</sub> or NO<sub>3</sub> with unknown VOCs, which were not detected or not identified by the GC system. However, the relative good agreement of the modeled and measured total OH reactivities leaves little room for missing reactive VOC. A similar situation was investigated by Di Carlo et al. (2004), who had found evidence for missing reactivity due to unmeasured reactive biogenic hydrocarbons in a forest and tried to explain unexpectedly high nighttime OH concentrations at the same location reported by Faloona et al. (2001). Di Carlo et al. (2004) supposed that some specific terpenes and sesquiterpenes, which are known to react faster with ozone than with OH, would be able to increase the OH production rate without a strong increase of  $k_{OH}$ , thus leading to an enhancement of the OH concentration.

The required concentration of an alkene ALK that would produce sufficient OH by ozonolysis in PRD or Beijing is given by Eq. (3).

$$[\text{ALK}] = \frac{\Delta P_{\text{RO}_x}}{k_{\text{O}_3+\text{ALK}}[\text{O}_3]Y_{\text{OH}}} \quad (3)$$

$\Delta P_{\text{RO}_x}$  denotes the additional RO<sub>x</sub> production rate of  $1 \text{ ppb h}^{-1}$ , while  $k_{\text{O}_3+\text{ALK}}$  and  $Y_{\text{OH}}$  represent the rate coefficient and OH yield of the ozonolysis, respectively. On the other side, the required VOC concentration is related to the concurrent increase of the OH reactivity ( $\Delta k_{\text{OH}}$ ) as follows:

$$[\text{ALK}] = \frac{\Delta k_{\text{OH}}}{k_{\text{OH}+\text{ALK}}}. \quad (4)$$

If we allow for an increase  $\Delta k_{\text{OH}}$  of  $3 \text{ s}^{-1}$  (which seems tolerable within the error margins of the modeled and measured  $k_{\text{OH}}$ ), then Eqs. (3) and (4) impose as a constraint for the alkene that the ratio  $k_{\text{OH}+\text{ALK}}/(k_{\text{O}_3+\text{ALK}}Y_{\text{OH}})$  must be in the range of  $(3-7) \times 10^5$  in PRD and about  $1 \times 10^5$  in Beijing. The above requirements would be fulfilled by highly reactive terpenoids like for example  $\delta$ -terpinene. It has rate constants for the reaction with OH and ozone of  $2.3 \times 10^{-10} \text{ cm}^3 \text{ s}^{-1}$  and  $1.8 \times 10^{-15} \text{ cm}^3 \text{ s}^{-1}$ , respectively, and an assumed OH yield of unity OH ( $Y = 1$ ) from ozonolysis (Atkinson and Arey, 2003). For typical nighttime O<sub>3</sub> concentrations ( $\approx 20 \text{ ppb}$ ) before midnight, about 500 ppt of

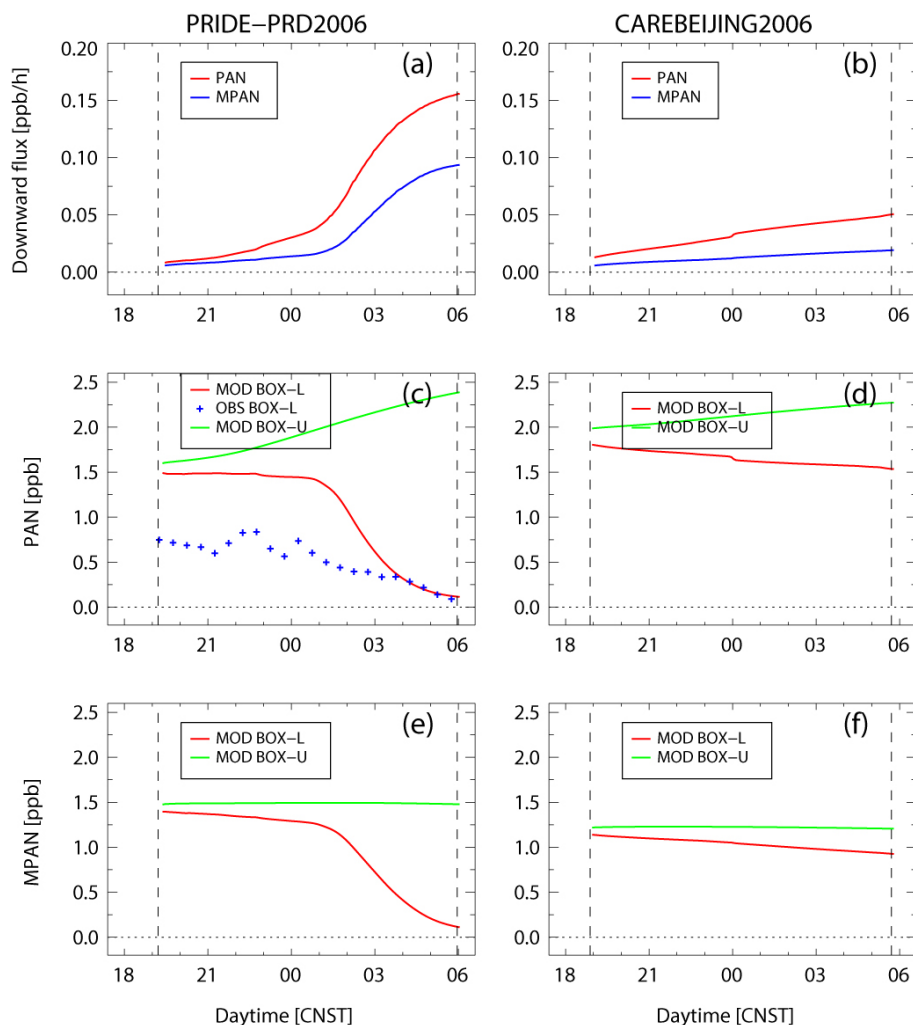


**Figure 12.** Estimated fluxes of PAN and MPAN transported downward from the residual layer to the stable surface layer during PRIDE-PRD2006 (a) and CAREBEIJING2006 (b). In the lower layer, the transported compounds decompose thermally and produce peroxy radicals at a rate approximately equal to the downward fluxes. The observed (if available) and modeled PAN and MPAN concentrations are shown in (c)–(f).

$\delta$ -terpinene would be enough to provide a primary RO<sub>x</sub> production rate of 1 ppb h<sup>-1</sup>. But this kind of species is so reactive towards O<sub>3</sub> that its lifetime would only be 10–30 min. Thus, without a strong local emission source (for which we have no direct evidence) it is unlikely that the concentration of such terpenoids can reach the required concentration levels.

#### 4.4.2 Vertical transport of radicals and radical reservoir species

The box model applied in this work implicitly assumes that the air near the ground where the field measurements were performed is homogeneously mixed. Such an assumption is reasonable for the daytime, when the planetary boundary-layer (PBL) is well mixed by turbulence up to 1–2 km height. In the night, however, a stable nocturnal boundary layer

(NBL) is formed at the bottom of the PBL. The NBL is a stable layer and is separated by a temperature inversion from the residual layer (RL) above which air of the mixed layer from the previous day is contained (Stull, 1988). In a conceptual model study, Geyer and Stutz (2004) have shown that distinct vertical profiles of RO<sub>x</sub> radicals can evolve in the NBL depending on the chemical and meteorological conditions, in particular if NO is emitted near the ground surface. Their model study reports OH maxima on the order of (1–2) × 10<sup>6</sup> cm<sup>-3</sup> in the lowest 2 m above ground and a decrease of the OH concentration within 10 m height to about 10<sup>5</sup> cm<sup>-3</sup>. Besides chemistry, the model results depend on the vertical transport of RO<sub>2</sub> and HNO<sub>4</sub> (as a HO<sub>2</sub> reservoir) and were found to be highly sensitive to changes in the atmospheric stability and NO surface emission.

The nocturnal HO<sub>x</sub> measurements in the present work were performed in environments with significant anthropogenic nighttime emission of NO (see Sect. 3.1) and at measurement heights (7 m) for which significant vertical radical gradients are predicted at night (Makar et al., 1999; Geyer and Stutz, 2004). Thus, it seems reasonable to apply a one-dimensional model to simulate the nocturnal radical concentrations in PRD and Yufa. However, the conditions (vertical profiles of trace gases, micrometeorological parameters, emission rates of NO and VOC) for implementation in a detailed model are not known. As a compromise, a simple one-dimensional model with only two boxes has been set up to investigate the sensitivity of the RO<sub>x</sub> radical budget to vertical transport at the measurement sites in PRD and Yufa. The lower box was chosen to represent a lower layer of 50 m depth and the upper box to represent the residual layer up to 1000 m height. The chemistry in each box is represented by RACM-MIM-GK, and the vertical exchange between the two boxes is parameterized by assuming diffusion with a momentum exchange coefficient  $K_z$ . The time dependent change of the trace gas concentrations in each each box can be described by Eq. (5).

$$\frac{\partial n_i}{\partial t} = n_a K_z \frac{\partial^2(C_i)}{\partial z^2} - R_i \quad (5)$$

$\partial n_i/\partial t$  is the rate of change of the number density  $n_i$  of the  $i$ th compound in the model box,  $n_a$  is the atmospheric number density,  $C_i$  is the mixing ratio of the  $i$ th compound in the model, and  $R_i$  denotes the contribution from the chemical reactions.

The model calculations were performed for the time from sunset to sunrise. For the lower layer, the initial values were taken from the base model (M0) result at sunset (Sect. 2.2), and net emission rates for long-lived species (i.e., NO, CO, C<sub>2</sub>–C<sub>12</sub> hydrocarbons) were introduced to resemble the measured concentrations. For the upper box, the initial values were taken from the base model M0 half an hour before sunset and no emissions were included. For the transport between the boxes,  $K_z$  was estimated by Eq. (6).

$$K_z = \frac{kzu_*}{\Phi\left(\frac{z}{L}\right)} \quad (6)$$

Here,  $k$  is the von Kármán constant (= 0.4),  $z$  is the height (= 50 m),  $u_*$  is the friction velocity,  $L$  is the Obukhov length, and  $\Phi$  is the dimensionless wind shear (Stull, 1988). The values for  $u_*$  and  $\Phi$  were calculated from three-dimensional wind measurements by an in situ ultrasonic anemometer that was operated at the height of the HO<sub>x</sub> measurements. The nocturnal temperature lapse rate was estimated to be  $-5.4 \text{ K km}^{-1}$  according to Fan et al. (2011). The observed temperature and temperature at 500 m are used as model constrains for the lower and upper boxes, respectively. For both PRIDE-PRD2006 and CAREBEIJING2006, the averaged  $K_z$  coefficients were calculated to be  $0.5 \text{ m}^2 \text{ s}^{-1}$  for 50 m height.

From the one-dimensional two-box model calculations, vertical transport rates can be determined. It is found that there is a weak direct transport of radicals from the upper into the lower layer, contributing on the order of  $10^{-5} \text{ ppb h}^{-1}$  of OH,  $10^{-3} \text{ ppb h}^{-1}$  of HO<sub>2</sub>, and  $10^{-2} \text{ ppb h}^{-1}$  of RO<sub>2</sub> in the lower layer. These contributions are negligible compared to the known chemical primary production rate of RO<sub>x</sub> (Table 4).

A significantly larger influence is expected from the transport of radical reservoir species. As pointed out in Sect. 4.3, some compounds like PANs and HNO<sub>4</sub> are expected to be in quasi-equilibrium with RO<sub>2</sub> and HO<sub>2</sub>, respectively, with high chemical interconversion rates (Figs. 6–9). Thus, a small perturbation of their thermal equilibria may have a significant impact on the abundance of RO<sub>x</sub>. Such a perturbation can result from continuous transport of reservoir species from one layer into another. In the case of the two campaigns in Yufa and PRD, the model predicts a downward flux of HNO<sub>4</sub> and PANs, which then thermally decompose into radicals in the lower layer. The HO<sub>2</sub> production following the downward transport of HNO<sub>4</sub> contributes less than  $0.01 \text{ ppb h}^{-1}$ , which is again negligible compared to the required additional RO<sub>x</sub> source of  $1 \text{ ppb h}^{-1}$ . However, downward transport and dissociation of peroxy acetic nitrate (PAN) and peroxymethacryloyl nitrate (MPAN), make a significant contribution, which after midnight reaches up to  $0.25 \text{ ppb h}^{-1}$  in PRD (see Fig. 12). This value is on the order of the known primary RO<sub>x</sub> production rates at nighttime in PRD and Yufa (Table 4). The relevance of this mechanism increases over the course of the night while NO increases in the lower layer due to emissions. The rising NO depletes peroxy radicals and thereby lowers the concentrations of PAN and MPAN. In contrast, the NO in the upper layer remains small owing to a lack of NO sources, and PAN and MPAN remain high. Thus, an increasing gradient develops between the upper and lower layers, leading to an increasing downward flux over the night. The modeled concentrations of the RACM-species PAN (=PAN and other higher saturated PANs) in the lower layer in PRD are comparable to measured values and show a similar temporal variation throughout the night. The simulated MPAN concentration level is also plausible as judged by the observed PAN-to-MPAN ratio (e.g., 6 to 10) reported for biogenically dominated air masses (Roberts et al., 1998). The role of entrainment of PAN from the top boundary of the upper layer is difficult to estimate without more detailed information about the nocturnal structure of the lower troposphere at the measurement sites. Such information is not available. Nevertheless, our analysis demonstrates that vertical transport is a possible candidate to explain at least part of the enhanced radical concentrations near the ground.

This process could eventually become the dominant nighttime RO<sub>x</sub> source, when ozone and NO<sub>3</sub> become more and more depleted by NO emissions in the lower layer, resulting in decreasing RO<sub>x</sub> formation from ozonolysis or VOC oxidation by NO<sub>3</sub>. In principle, downward transport of NO<sub>3</sub>



could also contribute to enhancing the RO<sub>x</sub> production in the lower layer, but the calculated downward transport rates are comparatively small ( $< 0.01 \text{ ppb h}^{-1}$ ). Although the vertical transport of the abovementioned compounds cannot account for the full amount of required primary RO<sub>x</sub> source strengths, the simple model demonstrates that vertical transport can play a significant role for the nighttime radicals near the ground, in agreement with the conclusions of the model study by Geyer and Stutz (2004). Thus, future field campaigns studying the nighttime chemistry would greatly benefit from additional measurement of vertical profiles of key species such as NO as well as of flux and micrometeorological measurements at different heights. The downward transport of PAN and its analogs would be especially important as an additional RO<sub>x</sub> radical source when the near-surface NO concentration becomes high.

## 5 Summary and conclusions

In two ground-based field campaigns, PRIDE-PRD2006 and CAREBEIJING2006, HO<sub>x</sub> radicals, total OH reactivity, and atmospheric trace gases were measured in summer 2006. One measurement site was located in a rural environment influenced by urban emissions in the Pearl River Delta (PRD), and the other site was in the suburban area Yufa near Beijing. In both campaigns, significant nighttime concentrations of radicals were observed under conditions with high total OH reactivities of about  $40\text{--}50 \text{ s}^{-1}$  in PRD and  $25 \text{ s}^{-1}$  in Yufa. For OH, the nocturnal concentrations were within the range of  $(0.5\text{--}3) \times 10^6 \text{ cm}^{-3}$ , implying a significant nighttime oxidation rate of pollutants on the order of several ppb per hour. A box model was used to compare the measured radical concentrations at night with the expectation from an established tropospheric chemistry mechanism (RACM-MIM-GK). The model was constrained by measured data for O<sub>3</sub>, HONO, NO, NO<sub>2</sub>, CO, VOC, water vapor, ambient temperature, pressure, and assumed deposition loss of model-generated species. For both field campaigns, the model is capable of reproducing the measured nighttime values of HO<sub>2</sub><sup>\*</sup> and  $k_{\text{OH}}$ , but underestimates in both cases the observed OH by about one order of magnitude. This feature is similar to results from other field studies that investigated the nighttime chemistry in urban areas and forests and found significantly more nighttime OH than expected from models (e.g., Tan et al., 2001). Noticeably, the large discrepancies between observed and modeled nighttime OH were generally found under conditions with high VOC reactivities. This finding and the recent discovery of a possibly VOC-related interference in the LIF OH instrument by the Penn State University group (Mao et al., 2012) raises the question of whether our nighttime observations in PRD and Yufa could be caused by an instrumental artifact. In previous field campaigns, nighttime OH concentrations measured by our LIF instrument were less or equal to a few  $10^5 \text{ cm}^{-3}$ , in agreement with model expect-

tations. Moreover, several instrumental tests and intercomparisons with independent measurement techniques, such as DOAS and CIMS, have not revealed any artifacts that could explain the nocturnal OH observation in PRD and Yufa. Nevertheless, further tests of our LIF instrument are planned in the laboratory and future field campaigns.

Sensitivity studies with the box model demonstrate that the OH discrepancy between measured and modeled nighttime OH in PRD and Yufa can be resolved, if an additional RO<sub>x</sub> production process (about  $1 \text{ ppb h}^{-1}$ ) and additional recycling (RO<sub>2</sub> → HO<sub>2</sub> → OH) with an efficiency equivalent to 1 ppb NO is assumed in the model. The additional recycling mechanism was also needed to reproduce the OH observations at the same locations during daytime for conditions with NO mixing ratios below 1 ppb. This could be an indication that the same missing process operates at day and night. Recent work has shown that isoprene peroxy radicals can undergo isomerization and regenerate HO<sub>2</sub> and OH without involvement of NO. Though isoprene was present in PRD and Yufa, its nighttime concentration was too small to explain the nocturnal OH. However, given the high abundance of other RO<sub>2</sub> at night, it appears desirable in future research to further investigate the potential of other RO<sub>2</sub> species for HO<sub>x</sub> regeneration.

The required primary source of RO<sub>x</sub> can be explained in principle by ozonolysis of terpenoids, which react faster with the given ozone than with OH in the nighttime atmosphere. Therefore, the modeled RO<sub>x</sub> concentrations can be increased without a large enhancement of  $k_{\text{OH}}$ , retaining the relative good agreement of the measured and modeled OH reactivity. However, the required mixing ratio of terpenoids, for example 500 ppt of  $\delta$ -terpinene, would need a strong local biogenic source, for which we have no direct evidence.

A more likely explanation for an additional RO<sub>x</sub> source is the vertical downward transport of radical reservoir species, e.g., PAN and MPAN, in the stratified nocturnal boundary layer and thermal decomposition of these species into radicals. This possibility proposed in a conceptual model paper by Geyer and Stutz (2004) was tested in this work using a simplified one-dimensional two-box model. In fact, a vertical gradient of RO<sub>x</sub> radicals, HNO<sub>4</sub>, PAN, and MPAN is expected to develop in the course of the night as a result of anthropogenic NO emissions at the ground, leading to a flux of these compounds from the air aloft into the atmospheric layer near the Earth's surface. While the transport of RO<sub>x</sub> and HNO<sub>4</sub> is too small to make an impact, the downward transport of PAN and MPAN is significant and reaches values after midnight up to  $0.3 \text{ ppb h}^{-1}$  in PRD, which are on the order of the known RO<sub>x</sub> production by ozonolysis and NO<sub>3</sub> reactions with VOC. This mechanism appears promising, but the model is highly simplified and not enough to explain the complete OH discrepancy.

In conclusion, the reasons for the high nighttime OH observations in PRD and Yufa are not completely understood. However, recent progress in laboratory and field studies and

the analysis of the present paper give directions for future work. Additional tests will be needed to quantify or exclude the possibility of measurement artifacts for OH. Further laboratory studies of the chemistry of VOC and its degradation products are needed, and in particular the potential of RO<sub>2</sub> to regenerate HO<sub>x</sub> needs further investigation. Finally, further studies of the nighttime chemistry in the lower troposphere will require more sophisticated one-dimensional models for analysis supported by field measurements probing the vertical distribution of trace gases and fluxes.

**Acknowledgements.** We thank the science teams of PRIDE-PRD2006 and CAREBEIJING2006. This work was supported by the National Natural Science Foundation of China (General Program: 41375124; Major Program: 21190052; and Innovative Research Group: 41121004), the Strategic Priority Research Program of the Chinese Academy of Sciences (grant no. XDB05010500), and the special fund of State Key Joint Laboratory of Environment Simulation and Pollution Control (13Z02ESPCP). The research was also supported by the Collaborative Innovation Center for Regional Environmental Quality. We thank Djuro Mihelcic for helpful discussions.

The service charges for this open access publication have been covered by a Research Centre of the Helmholtz Association.

Edited by: S. C. Liu

## References

- Atkinson, R. and Arey, J.: Gas-phase tropospheric chemistry of biogenic volatile organic compounds: a review, *Atmos. Environ.*, **37**, S197–S219, 2003.
- Brown, S. S., Ryerson, T. B., Wollny, A. G., Brock, C. A., Peltier, R., Sullivan, A. P., Weber, R. J., Dube, W. P., Trainer, M., Meagher, J. F., Fehsenfeld, F. C., and Ravishankara, A. R.: Variability in nocturnal nitrogen oxide processing and its role in regional air quality, *Science*, **311**, 67–70, 2006.
- Crounse, J. D., Paulot, F., Kjaergaard, H. G., and Wennberg, P. O.: Peroxy radical isomerization in the oxidation of isoprene, *Phys. Chem. Chem. Phys.*, **13**, 13 607–13 613, doi:10.1039/c1cp21330j, 2011.
- Di Carlo, P., Brune, W. H., Martinez, M., Harder, H., Leshner, R., Ren, X., Thornberry, T., Carroll, M. A., Young, V., Shepson, P. B., Riemer, D., Apel, E., and Campbell, C.: Missing OH Reactivity in a Forest: Evidence for Unknown Reactive Biogenic VOCs, *Science*, **304**, 722–724, 2004.
- Ehhalt, D. H.: Photooxidation of trace gases in the troposphere, *Phys. Chem. Chem. Phys.*, **1**, 5401–5408, 1999.
- Eisele, F. L., Mount, G. H., Tanner, D., Jefferson, A., Shetter, R., Harder, J. W., and Williams, E. J.: Understanding the production and interconversion of the hydroxyl radical during the Tropospheric OH Photochemistry Experiment, *J. Geophys. Res.*, **102**, 6457–6465, 1997.
- Emmerson, K. M. and Carslaw, N.: Night-time radical chemistry during the TORCH campaign, *Atmos. Environ.*, **43**, 3220–3226, 2009.
- Emmerson, K. M., Carslaw, N., Carpenter, L. J., Heard, D. E., Lee, J. D., and Pilling, M. J.: Urban atmospheric chemistry during the PUMA campaign 1: Comparison of modelled OH and HO<sub>2</sub> concentrations with measurements, *J. Atmos. Chem.*, **52**, 143–164, 2005.
- Faloona, I., Tan, D., Brune, W., Hurst, J., Barket, D., Couch, T. L., Shepson, P., Apel, E., Riemer, D., Thornberry, T., Carroll, M. A., Sillman, S., Keeler, G. J., Sagady, J., Hooper, D., and Pateron, K.: Nighttime observations of anomalously high levels of hydroxyl radicals above a deciduous forest canopy, *J. Geophys. Res.*, **106**, 24315–24333, 2001.
- Fan, S. J., Fan, Q., Yu, W., Luo, X. Y., Wang, B. M., Song, L. L., and Leong, K. L.: Atmospheric boundary layer characteristics over the Pearl River Delta, China, during the summer of 2006: measurement and model results, *Atmos. Chem. Phys.*, **11**, 6297–6310, doi:10.5194/acp-11-6297-2011, 2011.
- Finlayson-Pitts, B. J. and Pitts Jr., J. N.: Chemistry of the upper and lower atmosphere: Theory, experiments and applications, Academic Press, San Diego, 183–185, 2000.
- Fuchs, H., Bohn, B., Hofzumahaus, A., Holland, F., Lu, K. D., Nehr, S., Rohrer, F., and Wahner, A.: Detection of HO<sub>2</sub> by laser-induced fluorescence: calibration and interferences from RO<sub>2</sub> radicals, *Atmos. Meas. Tech.*, **4**, 1209–1225, doi:10.5194/amt-4-1209-2011, 2011.
- Fuchs, H., Dorn, H.-P., Bachner, M., Bohn, B., Brauers, T., Gomm, S., Hofzumahaus, A., Holland, F., Nehr, S., Rohrer, F., Tillmann, R., and Wahner, A.: Comparison of OH concentration measurements by DOAS and LIF during SAPHIR chamber experiments at high OH reactivity and low NO concentration, *Atmos. Meas. Tech.*, **5**, 1611–1626, doi:10.5194/amt-5-1611-2012, 2012.
- Fuchs, H., Hofzumahaus, A., Rohrer, F., Bohn, B., Brauers, T., Dorn, H.-P., Häsel, R., Holland, F., Kaminski, M., Li, X., Lu, K., Nehr, S., Tillmann, R., Wegener, R., and Wahner, A.: Experimental evidence for efficient hydroxyl radical regeneration in isoprene oxidation, *Nature Geosci.*, 2013.
- Garland, R. M., Yang, H., Schmid, O., Rose, D., Nowak, A., Achtert, P., Wiedensohler, A., Takegawa, N., Kita, K., Miyazaki, Y., Kondo, Y., Hu, M., Shao, M., Zeng, L. M., Zhang, Y. H., Andreae, M. O., and Pöschl, U.: Aerosol optical properties in a rural environment near the mega-city Guangzhou, China: implications for regional air pollution, radiative forcing and remote sensing, *Atmos. Chem. Phys.*, **8**, 5161–5186, doi:10.5194/acp-8-5161-2008, 2008.
- Garland, R. M., Schmid, O., Nowak, A., Achtert, P., Wiedensohler, A., Gunthe, S. S., Takegawa, N., Kita, K., Kondo, Y., Hu, M., Shao, M., Zeng, L. M., Zhu, T., Andreae, M. O., and Pöschl, U.: Aerosol optical properties observed during Campaign of Air Quality Research in Beijing 2006 (CAREBeijing-2006): Characteristic differences between the inflow and outflow of Beijing city air, *J. Geophys. Res.*, **114**, D00G04, doi:10.1029/2008JD010780, 2009.
- Geiger, H., Barnes, I., Bejan, I., Benter, T., and Spittler, M.: The tropospheric degradation of isoprene: an updated module for the regional atmospheric chemistry mechanism, *Atmos. Environ.*, **37**, 1503–1519, 2003.

- Geyer, A. and Stutz, J.: The vertical structure of OH-HO<sub>2</sub>-RO<sub>2</sub> chemistry in the nocturnal boundary layer: A one-dimensional model study, *J. Geophys. Res.*, 109, D16301, doi:10.1029/2003JD004425, 2004.
- Geyer, A., Bachmann, K., Hofzumahaus, A., Holland, F., Konrad, S., Klupfel, T., Patz, H. W., Perner, D., Mihelcic, D., Schafer, H. J., Volz-Thomas, A., and Platt, U.: Nighttime formation of peroxy and hydroxyl radicals during the BERLIOZ campaign: Observations and modeling studies, *J. Geophys. Res.*, 108, 8249, doi:10.1029/2001JD000656, 2003.
- Guenther, A.: Modeling biogenic volatile organic compound emissions to the atmosphere, in *Reactive Hydrocarbons in the Atmosphere*, edited by C. N. Hewitt, chap. 3, 97–118, Academic Press, 1999.
- Hofzumahaus, A., Aschmutat, U., Brandenburger, U., Brauers, T., Dorn, H.-P., Hausmann, M., Hessling, M., Holland, F., Plass-Dülmer, C., and Ehhalt, D. H.: Intercomparison of tropospheric OH measurements by different laser techniques during the POPCORN Campaign 1994, *J. Atmos. Chem.*, 31, 227–246, 1998.
- Hofzumahaus, A., Rohrer, F., Lu, K., Bohn, B., Brauers, T., Chang, C. C., Fuchs, H., Holland, F., Kita, K., Kondo, Y., Li, X., Lou, S., Shao, M., Zeng, L., Wahner, A., and Zhang, Y.: Amplified Trace Gas Removal in the Troposphere, *Science*, 324, 1702–1704, 2009.
- Holland, F., Aschmutat, U., Heßling, M., Hofzumahaus, A., and Ehhalt, D. H.: Highly time resolved measurements of OH during POPCORN using laser-induced fluorescence spectroscopy, *J. Atmos. Chem.*, 31, 205–225, 1998.
- Holland, F., Hofzumahaus, A., Schäfer, J., Kraus, A., and Pätz, H.-W.: Measurements of OH and HO<sub>2</sub> radical concentrations and photolysis frequencies during BERLIOZ, *J. Geophys. Res.*, 108, 8246, doi:10.1029/2001JD001393, 2003.
- Kanaya, Y., Cao, R. Q., Akimoto, H., Fukuda, M., Komazaki, Y., Yokouchi, Y., Koike, M., Tanimoto, H., Takegawa, N., and Kondo, Y.: Urban photochemistry in central Tokyo: 1. Observed and modeled OH and HO<sub>2</sub> radical concentrations during the winter and summer of 2004, *J. Geophys. Res.*, 112, D21312, doi:10.1029/2007JD008670, 2007.
- Kanaya, Y., Hofzumahaus, A., Dorn, H.-P., Brauers, T., Fuchs, H., Holland, F., Rohrer, F., Bohn, B., Tillmann, R., Wegener, R., Wahner, A., Kajii, Y., Miyamoto, K., Nishida, S., Watanabe, K., Yoshino, A., Kubistin, D., Martinez, M., Rudolf, M., Harder, H., Berresheim, H., Elste, T., Plass-Dülmer, C., Stange, G., Kl-effmann, J., Elshorbany, Y., and Schurath, U.: Comparisons of observed and modeled OH and HO<sub>2</sub> concentrations during the ambient measurement period of the HO<sub>x</sub> Comp field campaign, *Atmos. Chem. Phys.*, 12, 2567–2585, doi:10.5194/acp-12-2567-2012, 2012.
- Karl, M., Dorn, H.-P., Holland, F., Koppmann, R., Poppe, D., Rupp, L., Schaub, A., and Wahner, A.: Product study of the reaction of OH radicals with isoprene in the atmosphere simulation chamber SAPHIR, *J. Atmos. Chem.*, 55, 167–187, 2006.
- Lee, B. S. and Wang, J. L.: Concentration variation of isoprene and its implications for peak ozone concentration, *Atmos. Environ.*, 40, 5486–5495, 2006.
- Lelieveld, J., Butler, T. M., Crowley, J. N., Dillon, T. J., Fischer, H., Ganzeveld, L., Harder, H., Lawrence, M. G., Martinez, M., Taraborelli, D., and Williams, J.: Atmospheric oxidation capacity sustained by a tropical forest, *Nature*, 452, 737–740, 2008.
- Li, X., Brauers, T., Häseler, R., Bohn, B., Fuchs, H., Hofzumahaus, A., Holland, F., Lou, S., Lu, K. D., Rohrer, F., Hu, M., Zeng, L. M., Zhang, Y. H., Garland, R. M., Su, H., Nowak, A., Wiedensohler, A., Takegawa, N., Shao, M., and Wahner, A.: Exploring the atmospheric chemistry of nitrous acid (HONO) at a rural site in Southern China, *Atmos. Chem. Phys.*, 12, 1497–1513, doi:10.5194/acp-12-1497-2012, 2012.
- Liu, Y., Shao, M., Fu, L., Lu, S., Zen, L., and Tang, D.: Source profiles of volatile organic compounds (VOCs) measured in China: Part I, *Atmos. Environ.*, 42, 6247–6260, 2008.
- Lou, S., Holland, F., Rohrer, F., Lu, K., Bohn, B., Brauers, T., Chang, C., Fuchs, H., Häseler, R., Kita, K., Kondo, Y., Li, X., Shao, M., Zeng, L., Wahner, A., Zhang, Y., Wang, W., and Hofzumahaus, A.: Atmospheric OH reactivities in the Pearl River Delta – China in summer 2006: measurement and model results, *Atmos. Chem. Phys.*, 10, 11243–11260, doi:10.5194/acp-10-11243-2010, 2010.
- Lu, K. D. and Zhang, Y. H.: Observations of HO<sub>x</sub> Radical in Field Studies and the Analysis of Its Chemical Mechanism, *Prog. Chem.*, 22, 500–514, 2010.
- Lu, K. D., Zhang, Y. H., Su, H., Brauers, T., Chou, C. C., Hofzumahaus, A., Liu, S. C., Kita, K., Kondo, Y., Shao, M., Wahner, A., Wang, J. L., Wang, X. S., and Zhu, T.: Oxidant (O<sub>3</sub> + NO<sub>2</sub>) production processes and formation regimes in Beijing, *J. Geophys. Res.*, 115, D07 303, doi:10.1029/2009JD012714, 2010a.
- Lu, K. D., Zhang, Y. H., Su, H., Shao, M., Zeng, L. M., Zhong, L. J., Xiang, Y. R., Chang, C. C., Chou, C. K. C., and Wahner, A.: Regional ozone pollution and key controlling factors of photochemical ozone production in Pearl River Delta during summer time, *Sci. China Ser. B*, 53, 651–663, 2010b.
- Lu, K. D., Rohrer, F., Holland, F., Fuchs, H., Bohn, B., Brauers, T., Chang, C. C., Häseler, R., Hu, M., Kita, K., Kondo, Y., Li, X., Lou, S. R., Nehr, S., Shao, M., Zeng, L. M., Wahner, A., Zhang, Y. H., and Hofzumahaus, A.: Observation and modelling of OH and HO<sub>2</sub> concentrations in the Pearl River Delta 2006: a missing OH source in a VOC rich atmosphere, *Atmos. Chem. Phys.*, 12, 1541–1569, doi:10.5194/acp-12-1541-2012, 2012.
- Lu, K. D., Hofzumahaus, A., Holland, F., Bohn, B., Brauers, T., Fuchs, H., Hu, M., Häseler, R., Kita, K., Kondo, Y. and Li, X., Lou, S. R., Oebel, A., Shao, M., Zeng, L. M., Wahner, A., Zhu, T., Zhang, Y. H., and Rohrer, F.: Missing OH source in a suburban environment near Beijing: observed and modelled OH and HO<sub>2</sub> concentrations in summer 2006, *Atmos. Chem. Phys.*, 13, 1057–1080, doi:10.5194/acp-13-1057-2013, 2013.
- Makar, P. A., D.Fuentes, J., Wang, D., Staebler, R. M., and Wiebe, H. A.: Chemical processing of biogenic hydrocarbons within and above a temperate deciduous forest, *J. Geophys. Res.*, 104, 3581–3603, 1999.
- Mao, J., Ren, X., Chen, S., Brune, W. H., Chen, Z., Martinez, M., Harder, H., Lefter, B., Rappenglück, B., Flynn, J., and Leuchner, M.: Atmospheric oxidation capacity in the summer of Houston 2006: Comparison with summer measurements in other metropolitan studies, *Atmos. Environ.*, 44, 4107–4115, doi:10.1016/j.atmosenv.2009.01.013, 2010.
- Mao, J., Ren, X., Zhang, L., Van Duin, D. M., Cohen, R. C., Park, J.-H., Goldstein, A. H., Paulot, F., Beaver, M. R., Crouse, J. D., Wennberg, P. O., DiGangi, J. P., Henry, S. B., Keutsch, F. N., Park, C., Schade, G. W., Wolfe, G. M., Thornton, J. A., and Brune, W. H.: Insights into hydroxyl measurements and atmo-

- spheric oxidation in a California forest, *Atmos. Chem. Phys.*, 12, 8009–8020, doi:10.5194/acp-12-8009-2012, 2012.
- Martinez, M., Harder, H., Kovacs, T. A., Simpas, J. B., Bassis, J., Leshner, R., Brune, W. H., Frost, G. J., Williams, E. J., Stroud, C. A., Jobson, B. T., Roberts, J. M., Hall, S. R., Shetter, R. E., Wert, B., Fried, A., Alicke, B., Stutz, J., Young, V. L., White, A. B., and Zamora, R. J.: OH and HO<sub>2</sub> concentrations, sources, and loss rates during the Southern Oxidants Study in Nashville, Tennessee, summer 1999, *J. Geophys. Res.*, 108, 4617, doi:10.1029/2003JD003551, 2003.
- Matsui, H., Koike, M., Kondo, Y., Takegawa, N., Kita, K., Miyazaki, Y., Hu, M., Chang, S. Y., Blake, D. R., Fast, J. D., Zaveri, R. A., Streets, D. G., Zhang, Q., and Zhu, T.: Spatial and temporal variations of aerosols around Beijing in summer 2006: Model evaluation and source apportionment, *J. Geophys. Res.*, 114, D00G13, doi:10.1029/2008JD010906, 2009.
- Mihelcic, D., Klemp, D., Musgen, P., Patz, H. W., and Volzthomas, A.: Simultaneous Measurements of Peroxy and Nitrate Radicals at Schauinsland, *J. Atmos. Chem.*, 16, 313–335, 1993.
- Monks, P. S., Granier, C., Fuzzi, S., Stohl, A., Williams, M., Aki-moto, H., Ammani, M., Baklanov, A., Baltensperger, U., Bey, I., Blake, N., Blake, R., Carslaw, K., Cooper, O., Dentener, F., Fowler, D., Fragkou, E., Frost, G., Generoso, S., Ginoux, P., Grewe, V., and H. C. Hansson, A. G., Henne, S., Hjorth, J., Hofzumahaus, A., Huntrieser, H., Isaksen, I. S. A., Jenkin, M. E., Kaiser, J., Kanakidou, M., Klimont, Z., Kulmala, M., Laj, P., Lawrence, M., Lee, J., Liousse, C., Maione, M., McFiggans, G., Metzger, A., Mieville, A., Moussiopoulos, N., Orlando, J., O'Dowd, C., Palmer, P., Parrish, D., Petzold, A., Platt, U., Pöschl, U., Prévôt, A. S. H., Reeves, C. E., Reimann, S., Rudich, Y., Sellegri, K., Steinbrecher, R., Simpson, D., ten Brink, H., Theloke, J., van der Werf, G. R., Vautard, R., Vestreng, V., Vlachokostas, C., and von Glasow, R.: Atmospheric Composition Change - Global and Regional Air Quality, *Atmos. Environ.*, 43, 5268–5350, 2009.
- Peeters, J. and Müller, J.-F.: HO<sub>x</sub> radical regeneration in isoprene oxidation via peroxy radical isomerisations. II: experimental evidence and global impact, *Phys. Chem. Chem. Phys.*, 12, 14227–14235, doi:10.1039/c0cp00811g, 2010.
- Peeters, J., Nguyen, T. L., and Vereecken, L.: HO<sub>x</sub> radical regeneration in the oxidation of isoprene, *Phys. Chem. Chem. Phys.*, 11, 5935–5939, 2009.
- Platt, U., Rateike, M., Junkermann, W., Rudolph, J., and Ehhalt, D. H.: New tropospheric OH measurements, *J. Geophys. Res.*, 93, 5159–5166, 1988.
- Platt, U. F., Winer, A. M., Biermann, H. W., Atkinson, R., and Pitts, J. N.: Measurement of Nitrate Radical Concentrations in Continental Air, *Environ. Sci. Technol.*, 18, 365–369, 1984.
- Ren, X., Harder, H., Martinez, M., Leshner, R. L., Oligier, A., Simpas, J. B., Brune, W. H., Schwab, J. J., Demerjian, K. L., He, Y., Zhou, X., and Gao, H.: OH and HO<sub>2</sub> Chemistry in the urban atmosphere of New York City, *Atmos. Environ.*, 37, 3639–3651, 2003.
- Ren, X. R., Harder, H., Martinez, M., Leshner, R. L., Oligier, A., Shirley, T., Adams, J., Simpas, J. B., and Brune, W. H.: HO<sub>x</sub> concentrations and OH reactivity observations in New York City during PMTACS-NY2001, *Atmos. Environ.*, 37, 3627–3637, 2003a.
- Ren, X. R., Harder, H., Martinez, M., Leshner, R. L., Oligier, A., Simpas, J. B., Brune, W. H., Schwab, J. J., Demerjian, K. L., He, Y., Zhou, X. L., and Gao, H. G.: OH and HO<sub>2</sub> chemistry in the urban atmosphere of New York City, *Atmos. Environ.*, 37, 3639–3651, 2003b.
- Ren, X. R., Harder, H., Martinez, M., Faloona, I. C., Tan, D., Leshner, R. L., Di Carlo, P., Simpas, J. B., and Brune, W. H.: Interference testing for atmospheric HO<sub>x</sub> measurements by laser-induced fluorescence, *J. Atmos. Chem.*, 47, 169–190, 2004.
- Roberts, J. M., Williams, J., Baumann, K., Buhr, M. P., Goldan, P. D., Holloway, J., Hubler, G., Kuster, W. C., McKeen, S. A., Ryerson, T. B., Trainer, M., Williams, E. J., Fehsenfeld, F. C., Bertman, S. B., Nouaime, G., Seaver, C., Grodzinsky, G., Rodgers, M., and Young, V. L.: Measurements of PAN, PPN, and MPAN made during the 1994 and 1995 Nashville Intensives of the Southern Oxidant Study: Implications for regional ozone production from biogenic hydrocarbons, *J. Geophys. Res.-Atmos.*, 103, 22473–22490, 1998.
- Sadanaga, Y., Matsumoto, J., and Kajii, Y.: Photochemical reactions in the urban air: Recent understandings of radical chemistry, *J. Photochem. Photobiol.*, 4, 85–104, 2003.
- Schlosser, E., Bohn, B., Brauers, T., Dorn, H., Fuchs, H., Häsel, R., Hofzumahaus, A., Holland, F., Rohrer, F., Rupp, L. O., Siese, M., Tillmann, R., and Wahner, A.: Intercomparison of Two Hydroxyl Radical Measurement Techniques at the Atmosphere Simulation Chamber SAPHIR, *J. Atmos. Chem.*, 56, 187–205, doi:10.1007/s10874-006-9049-3, 2007.
- Schlosser, E., Brauers, T., Dorn, H.-P., Fuchs, H., Häsel, R., Hofzumahaus, A., Holland, F., Wahner, A., Kanaya, Y., Kajii, Y., Miyamoto, K., Nishida, S., Watanabe, K., Yoshino, A., Kubistin, D., Martinez, M., Rudolf, M., Harder, H., Berresheim, H., Elste, T., Plass-Dülmer, C., Stange, G., and Schurath, U.: Technical Note: Formal blind intercomparison of OH measurements: results from the international campaign HOxComp, *Atmos. Chem. Phys.*, 9, 7923–7948, doi:10.5194/acp-9-7923-2009, 2009.
- Shao, M., Czapiewski, V., Heiden, A., Kobel, K., Komenda, M., Koppmann, R., and Wildt, J.: Volatile organic compound emissions from Scots pine: Mechanisms and description by algorithms, *J. Geophys. Res.*, 106, 20483–20491, 2001.
- Shirley, T. R., Brune, W. H., Ren, X., Mao, J., Leshner, R., Cardenas, B., Volkamer, R., Molina, L. T., Molina, M. J., Lamb, B., Velasco, E., Jobson, T., and Alexander, M.: Atmospheric oxidation in the Mexico City Metropolitan Area (MCMA) during April 2003, *Atmos. Chem. Phys.*, 6, 2753–2765, doi:10.5194/acp-6-2753-2006, 2006.
- Sillman, S., Carroll, M. A., Thornberry, T., Lamb, B. K., Westberg, H., Brune, W. H., Faloona, I., Tan, D., Shepson, P. B., Sumner, A. L., Hastie, D. R., Mihele, C. M., Apel, E. C., Riemer, D. D., and Zika, R. G.: Loss of isoprene and sources of nighttime OH radicals at a rural site in the United States: Results from photochemical models, *J. Geophys. Res.*, 107, 4043, doi:10.1029/2001JD000449, 2002.
- Stull, R. B.: *An Introduction to Boundary Layer Meteorology*, Kluwer Academic Publishers, 440–465, 1988.
- Takegawa, N., Miyakawa, T., Kondo, Y., Jimenez, J. L., Worsnop, D. R., and Fukuda, M.: Seasonal and diurnal variations of sub-micron organic aerosol in Tokyo observed using the Aerodyne Aerosol Mass Spectrometer, *J. Geophys. Res.*, 111, D11206, doi:10.1029/2005JD006515, 2006.
- Tan, D., Faloona, I., Simpas, J. B., Brune, W., and Shepson, P. B.: HO<sub>x</sub> budgets in a deciduous forest: Results from the PROPHET

- summer 1998 campaign, *J. Geophys. Res.*, 106, 24407–24427, 2001.
- Wang, B., Shao, M., Roberts, J. M., Yang, G., Yang, F., Hu, M., Zeng, L. M., Zhang, Y. H., and Zhang, J. B.: Ground-based on-line measurements of peroxyacetyl nitrate (PAN) and peroxypropionyl nitrate (PPN) in the Pearl River Delta, China, *International J. Environ. Anal. Chem.*, 90, 548–559, 2010.
- Wang, J. L., Wang, C. H., Lai, C. H., Chang, C. C., Liu, Y., Zhang, Y., Liu, S., and Shao, M.: Characterization of ozone precursors in the Pearl River Delta by time series observation of non-methane hydrocarbons, *Atmos. Environ.*, 42, 6233–6246, doi:10.1016/j.atmosenv.2008.01.050, 2008.
- Whalley, L. K., Edwards, P. M., Furneaux, K. L., Goddard, A., Ingham, T., Evans, M. J., Stone, D., Hopkins, J. R., Jones, C. E., Karunaharan, A., Lee, J. D., Lewis, A. C., Monks, P. S., Moller, S. J., and Heard, D. E.: Quantifying the magnitude of a missing hydroxyl radical source in a tropical rainforest, *Atmos. Chem. Phys.*, 11, 7223–7233, doi:10.5194/acp-11-7223-2011, 2011.
- Xiao, R., Takegawa, N., Kondo, Y., Miyazaki, Y., Miyakawa, T., Hu, M., Shao, M., Zeng, L. M., Hofzumahaus, A., Holland, F., Lu, K., Sugimoto, N., Zhao, Y., and Zhang, Y. H.: Formation of submicron sulfate and organic aerosols in the outflow from the urban region of the Pearl River Delta in China, *Atmos. Environ.*, 43, 3754–3763, 2009.
- Xie, X., Shao, M., Liu, Y., Lu, S. H., Chang, C. C., and Chen, Z. M.: Estimate of initial isoprene contribution to ozone formation potential in Beijing, China, *Atmos. Environ.*, 42, 6000–6010, 2008.